2016

Towards an Understanding of the Role of Cation Packaging on DNA Protection from Oxidative Damage

Cody E. Gay
University of Kentucky, cody.gay@uky.edu
Digital Object Identifier: http://dx.doi.org/10.13023/ETD.2016.348

STUDENT AGREEMENT:

I represent that my thesis or dissertation and abstract are my original work. Proper attribution has been given to all outside sources. I understand that I am solely responsible for obtaining any needed copyright permissions. I have obtained needed written permission statement(s) from the owner(s) of each third-party copyrighted matter to be included in my work, allowing electronic distribution (if such use is not permitted by the fair use doctrine) which will be submitted to UKnowledge as Additional File.

I hereby grant to The University of Kentucky and its agents the irrevocable, non-exclusive, and royalty-free license to archive and make accessible my work in whole or in part in all forms of media, now or hereafter known. I agree that the document mentioned above may be made available immediately for worldwide access unless an embargo applies.

I retain all other ownership rights to the copyright of my work. I also retain the right to use in future works (such as articles or books) all or part of my work. I understand that I am free to register the copyright to my work.

REVIEW, APPROVAL AND ACCEPTANCE

The document mentioned above has been reviewed and accepted by the student's advisor, on behalf of the advisory committee, and by the Director of Graduate Studies (DGS), on behalf of the program; we verify that this is the final, approved version of the student's thesis including all changes required by the advisory committee. The undersigned agree to abide by the statements above.

Cody E. Gay, Student

Dr. Jason DeRouchey, Major Professor

Dr. Mark Lovell, Director of Graduate Studies

TOWARDS AN UNDERSTANDING OF THE ROLE OF CATION PACKAGING ON DNA PROTECTION FROM OXIDATIVE DAMAGE

THESIS

A thesis submitted in partial fulfillment of the
requirements for the degree of Master of Science in the
College of Arts and Sciences
at the University of Kentucky

By

Cody Edward Gay

Lexington, Kentucky

Director: Dr. Jason DeRouchey, Assistant Professor of Chemistry

Lexington, Kentucky

2016

ABSTRACT OF THESIS

TOWARDS AN UNDERSTANDING OF THE ROLE OF CATION PACKAGING ON DNA PROTECTION FROM OXIDATIVE DAMAGE

In sperm chromatin, DNA exists in a highly condensed state reaching a final volume roughly twenty times that of a somatic nucleus. For the vast majority (>90%) of sperm DNA in mammals, somatic-like histones are first replaced by transition proteins which in turn are replaced by arginine-rich protamines. This near crystalline organization of the DNA in mature sperm is thought crucial for both the transport and protection of genetic information since all DNA repair mechanisms are shut down. Recent studies show that increased DNA damage is linked to dysfunctions in replacing histones with protamines resulting in mispackaged DNA. This increased DNA damage correlates not only to infertility but also impacts normal embryonic development. This damage is currently poorly characterized, but is known to involve oxidative base damage by reactive oxygen species (ROS).

Using a variety of biophysical methods, the effect of DNA condensation by polycations on the on free radical access and DNA damage in the packaged state was investigated. In Chapter 2, gel electrophoresis was used to quantify the ability of free radicals to damage both unpackaged and packaged DNA. DNA condensed by polycations shows significantly reduced levels of indirect damage from exposure to free radicals. Combining previous work on packaging density, it is also shown that differences in the packaged state, even by a few Angstroms, can result in significantly different degrees of damage to the DNA. In Chapter 3, we investigate the effects of protamine concentration on the ability to condense and protect DNA. Insufficient protamination is known to be a potential source of protamine dysfunction in mammalian sperm chromatin. Using gel retardation assays and UV-Vis studies, we examined the ability for DNA to condense with protamine at varying nitrogen to phosphate (N:P) charge ratios. Initial results on damage as a function of N:P are also discussed. Future work will more quantitatively determine the interrelationship between DNA packaging densities and the resulting accessibility of DNA to reactive oxygen species (ROS).

KEYWORDS: Protamine, DNA, oxidative damage, gel electrophoresis

Cody Edward Gay

July 28, 2015

TOWARDS AN UNDERSTANDING OF THE ROLE OF CATION PACKAGING ON DNA PROTECTION FROM OXIDATIVE DAMAGE

By

Cody Gay

Dr. Jason DeRouchey
Director of Thesis

Dr. Mark Lovell
Director of Graduate Studies

July 28, 2015

ACKNOWLEDGEMENTS

I would like to acknowledge and show deep appreciation to my advisor Dr. Jason DeRouchey for his assistance in getting me to this point. His guidance and patience throughout my graduate career has proven to be invaluable. He has been a great mentor and leader. In addition, I would like to thank the faculty and staff in the department of chemistry at the University of Kentucky for their help and support. Finally, I thank all of my group members who have supported me and provided a network to share ideas and troubleshoot problems.

TABLE OF CONTENTS

List of Figures

CHAPTER 1: INTRODUCTION

In this study, we are interested in understanding the effects of DNA packaging by polycations on the ability to protect nucleic acids from indirect damage by free radical. In this introductory chapter, we will briefly describe the difference between the normal somatic packaging of DNA and protamine-packaging of DNA in sperm chromatin. The formation of mature sperm during spermatogenesis is also briefly discussed. Lastly, we will discuss briefly what is known about reactive oxidative species (ROS) damage of DNA and its implications to reproductive function in sperm.

1.1 Chromatin Structure

Understanding how DNA is packaged in sperm chromatin has important consequences for cell biology as well as fertility. To better understand our approach towards investigating the protection that DNA packaging offers, we will first discuss the DNA packaging differences between a somatic cell and a sperm cell.

1.1.1 Sperm vs Somatic Cells

One of the most contrasting differences between a typical sperm cell and a somatic cell is their size. A sperm cell is much more compact when compared to a

somatic cell. Whereas a somatic cell can be full of many different organelles, with the exact identity of each organelle varying depending on the cell type, fully developed spermatozoa only consists of highly packaged DNA in the head and a tail to give motility. A sperm cell nucleus can be as much as forty times smaller than a somatic cell nucleus [1]. In order to achieve such high DNA packaging density in sperm chromatin, small basic proteins called protamines are used to condense the DNA into nearly crystalline arrays. This is compared to the markedly bulkier packaging of DNA in a somatic cell as shown in Figure 1.1 [2].

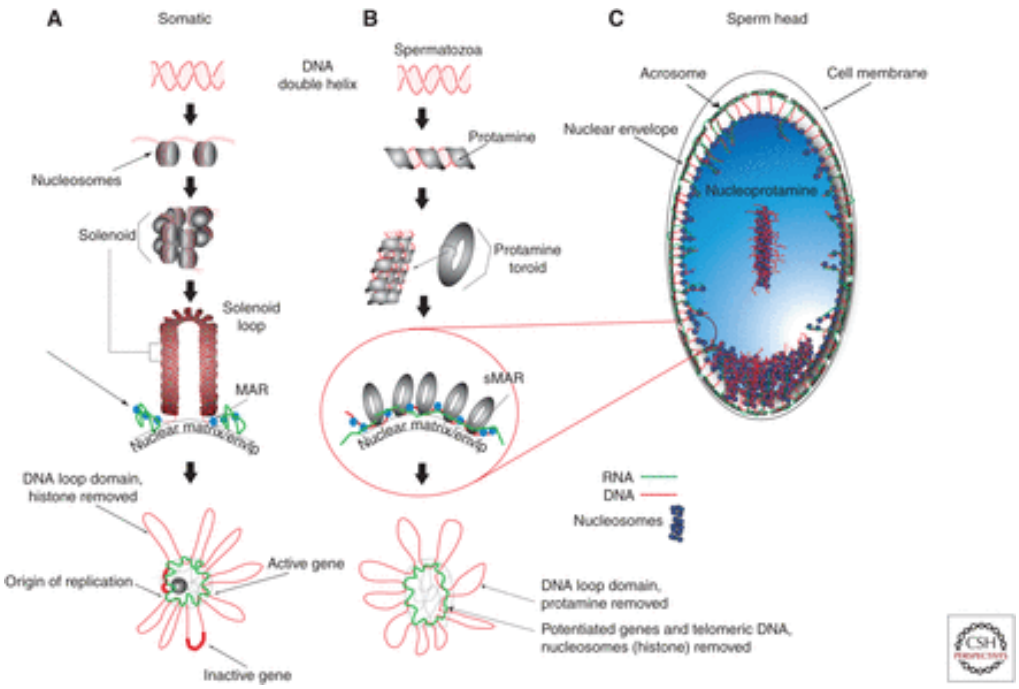

Figure 1.1 Model for sperm protamine and histone DNA packaging Reprinted from Miller, D., *Confrontation, Consolidation, and Recognition: The Oocyte's Perspective on the Incoming Sperm.* Cold Spring Harbor Perspectives in Medicine, 2015. **5**(8).[3]

Complexes of DNA and protein in eukaryotic cells are called chromatin. In the somatic cell, DNA is first packaged into nucleosomes, in which the DNA is wrapped around an octamer of histones, every two hundred base pairs [4]. These nucleosomes are then coiled into a solenoid or "30 nm fiber". The solenoid loops are associated with the nuclear matrix by matrix attachment regions (MAR) [3]. The solenoids are further organized to form the large chromatid and ultimately the classic x-shaped structure of the metaphase chromosome. Sperm nuclei, however, do not have the volume for this type of packaging. Instead of the DNA wrapping around histones, the DNA is condensed by arginine-rich protamines. It is thought that protamine is small enough to lie in the major or minor grooves of DNA. Here the number of highly positively charged residues on the protamine is sufficient to completely neutralize the negative phosphate groups on the DNA. The side by side linear packaging of DNA forms a toroid shape, which are better able to pack the DNA into the small volume required. The toroids vary in diameter from 50 to 100 nm and are estimated to contain roughly 50 kbp of DNA per toroid. These toroids are further organized inside the sperm head through links by matrix attachment regions (MARs) which bind them to the nuclear matrix [5]. While approximately 90% of sperm DNA is packaged by protamines, there are still specific regions that retain the histone packaging of somatic cells. While not fully understood, it is thought that the minor fraction of histone packaged DNA sperm may influence the order that genes are repacked or expressed following fertilization. Additionally these protamine and non-protamine regions in mature sperm may provide insight into the many transcription processes occurring in the course of chromatin remodeling during spermatogenesis [6].

1.1.2 Histone vs Protamine packaging

The key difference between a somatic cell and a sperm is the packaging, as previously discussed. The proteins that actually condense the DNA are of major interest and their differences are the key reason that the packaging volumes are so different. A typical histone protein is alkaline and is chiefly found in somatic cells. Core histones are conserved proteins. That is to say that there are not many differences in histones of different species [7]. Core histones all feature a helix turn helix motif, and long tails. These tails are where post-transitional modifications take place, and help signal unwinding. Histones alkalinity comes from its number of basic amino acid residues, primarily lysine amino acids many of which are found in the tails.

In contrast, DNA within sperm cell nuclei are packaged by highly basic, arginine-rich proteins called protamines with the main function of condensing DNA into a near crystalline density. While there is evidence that protamines evolved from H1-like histones, for most protamines the charge is nearly all from arginine residues with little to no lysine residues. [8] Protamines in eutherian mammals also contain multiple cysteine residues capable of forming disulfide bridges that are thought crucial to chromatin complex stabilization in the late stages of sperm maturation. Protamines in other animals including birds, reptiles and fish lack these cysteines. Comparisons of protamine sequence between fish and mammals show that while the arginine-rich regions are highly conserved while the remainder of the sequences exhibit considerable variation [8].

Another key difference between protamine and histones is their primary structure. As mentioned before, histones will commonly have certain defined primary structures in common with one another. Protamines, due to the high amount of highly charged basic residues, have no such primary structure in solution prior to bonding with DNA.

1.1.3 DNA Condensation in vitro

DNA condensation is defined as the collapse of DNA chains into compact, orderly particles containing only a few molecules [9]. DNA *in vitro* will spontaneously compress in the presence of counterions with a charge of +3 or higher. Polycation-DNA assemblies often form torodial or rod-like particles where DNA helices are set parallel to one another in a hexagonal lattice inside the condensate. While there is more to condensing DNA than simple electrostatic attractions between cations and DNA, the nature of the cation represents a large driving force in DNA condensation. Protamine-DNA complexes package more similarly to smaller multivalent cations than those of histone-DNA complexes [10]. One of the distinguishing characteristics of protamine is the presence of several charged basic amino acids, notably arginine. Arginine at physiological pH has a positive charge. The high valency of the protamines creates attractive forces for the DNA to bind to the protamine and condense. The size of the DNA seems to not affect the dimensions after compaction, provided the ratio of DNA to compression protein remains similar. There does seem to be a minimum size, if the DNA is too short (< 400 bp) it will fail to condense into orderly particles [9].

Studies by DeRouchey and others have shown that reconstituted protamine-DNA results in hexagonal packaging similar to other polycation-DNA complexes as well as the packing found in the toroidal structure of natural sperm chromatin [11-13]. Changes in the cation chemistry alter the attractive and repulsive intermolecular forces resulting in variations of the packaging density achieved in polycation-DNA complexes. Upon condensation, the resulting compacted structures have well-defined equilibrium surface separations of the DNA double helices of typically 7 - 15 Å, depending on the identity of the condensing ion. DeRouchey recently showed that the non-charged residues of protamine contribute primarily to the repulsive intermolecular forces reducing the compaction energies and packaging densities achieved in protamine-DNA compared to polyarginine-DNA [12]. It was also shown that protamine-DNA and polyarginine-DNA are able to package DNA considerably tighter than polylysine-DNA complexes due presumably to hydration differences between arginines and lysines.

1.2 Formation of spermatozoa

Spermatogenesis, the formation of sperm, takes place in the testis. The entire production cycle can last anywhere from 74 to 120 days and is depicted in Figure 1.2 [14, 15]. During this time the DNA inside is particularly vulnerable. Due to the close packaging of DNA in the sperm, there is not enough space in the major groove of the DNA helix for repair proteins to bind and thus normal DNA repair mechanisms are shut down. In this state, any damage inflicted on the DNA will accumulate until it reaches the

egg. If the sperm fails to reach the egg in this amount of time, the sperm cell is broken down and absorbed by the male body.

The process of spermatogenesis, depicted in Figure 1.2, begins with a standard mitosis of a progenitor spermatogonium. The end result of this mitotic division is referred to as a primary spermatocyte. Meiosis separates the chromosomes in the primary spermatocyte to form a secondary spermatocyte. A second round of meiosis gives way to spermatids, haploid precursors to functional sperm. These spermatids are transformed into true sperm by way of spermiogenesis. As a result of this process the amount of cytoplasm is reduced and the end result is spermatozoa, formed mature sperm.

1.2.1 Function of protamine in spermatogenesis

While protamines were discovered a long time ago, their function in sperm is still not yet fully understood. Two of the most commonly proposed functions of protamines are to facilitate the formation of a compact and hydrodynamic nucleus to enable efficient transfer of the spermatozoa and to protect paternal genetic information from potential damages by making it inaccessible to nucleases or mutagens during the transit process before fertilization. In addition, potential additional functions proposed include (i) competition and removal of transcription factors and other proteins to generate a blank paternal genetic message (ii) imprinting of the paternal genome to confer an epigenetic

mark, (iii) act as a checkpoint molecule during spermiogenesis, (iv) have some role in the fertilized ova [16]. For much of the work in this thesis, we will focus on the function of protamines to protect DNA from mutagens; namely free radical species.

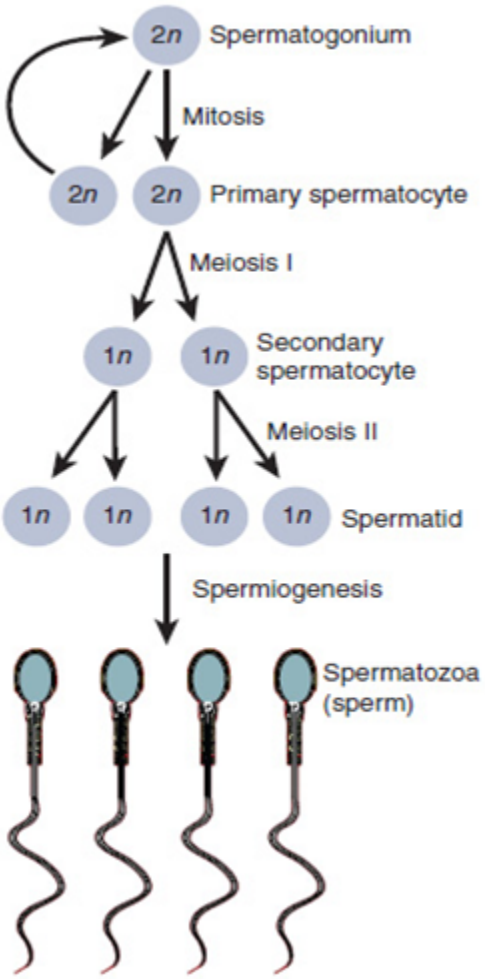

Figure 1.2 Spermatogenesis. The cell moves from spermatogonium to primary spermatocytes to secondary spermatocytes. From this point the cells transform to spermatid where they undergo spermiogenesis to form functional spermatozoa [17].

1.2.2 Male Infertility

A recent finding has that up to 15 percent of couples are infertile. This definition of infertility means that they have not been able to conceive a child after attempting regularly for a year or longer. In half of these couples, male infertility is believed to be the cause [18]. There can be a large number of factors that influence male infertility. These variables can be low sperm count, low motility, morphology, environmental factors, illnesses, or lifestyle choices. Simply put, male fertility relies on the production of enough healthy sperm having the functionality to reach and penetrate the egg. By better understanding the underlying causes of infertility, further research endeavors can be made to treat this underlying problems.

1.2.3 Common Causes

One of the most common problems in male fertility is having a low sperm count. Should the sperm count be low in the semen, it decreases the odds that one of the sperm will fertilize the egg. A low sperm count indicates a lower cell count per mL of seminal fluid. Sperm count can be affected by wide number of issues including overheating, radiation/x-rays, heavy metal exposure, illness, or injury can all negatively affect the ability to produce and maintain a high sperm count. All of the listed reasons can also influence the motility of sperm as well. Should enough sperm lose the ability to travel to

the egg on their own the number of possible interactions between the sperm and the egg will drop to an infertile level. Aberrant sperm are also a common cause. These malformed cells can have significant defects in their structure that compromise the sperms ability to travel unimpeded through the tubules. Any change to the sperm structure could dampen its effectiveness, for example an extra head could lead a rejection of the sperm by the egg. Tails can also become “bent” leading to the inability to travel in a straight line and not reach the egg.

Many environmental factors can influence the sperm quality as well. Overheating is one of the more common elements that are detrimental to male fertility. Sperm have a slightly lower heat tolerance than the rest of the body, so are more affected by such temperature increases. Some of the more easily resolved problems are wearing tight undergarments, working on a laptop computer for long periods, or sitting for extended durations. All of these can possibly increase the temperature in the scrotum and should be avoided. Other lifestyle choices that can influence male fertility could be alcohol use and tobacco smoking. Men that smoke tobacco have been proven to have abnormal protamine levels compared to those that do smoke [19].

1.2.4 ROS and Oxidative stress

Normal male fertility parameters including sperm count, motility and morphology are typically examined when looking into infertility causes. In addition, DNA fragmentation is gaining more attention as a significant cause of fertility issues in unexplained infertility [20, 21]. Sperm DNA damage levels have strong correlations with almost all fertility check points, however most conventional semen analysis does not assess for sperm damage due to difficulties to perform such analysis in a clinic setting. Ideally DNA fragmentation should be reduced as much as possible and thought to correlate to proper packaging of the sperm chromatin during spermatogenesis. The intensity of DNA fragmentation has a negative correlation with successful pregnancy in both natural and assisted conceptions. Furthermore, increased levels of damage are correlated with higher levels of spontaneous abortion as well as higher levels of genetic disease in the offspring [22-24]. The biggest factors in the level of DNA fragmentation in spermatozoa are reactive oxygen species (ROS) and oxidative stress. Typically assisted reproductive technologies (ARTs), like in-vitro fertilization, can help bypass infertility factors. With oxidative damage, the harm caused to the sperm may lead to rejection by the egg, resulting in a failed conception. It has been estimated over 48.5 million couples worldwide have used ARTs accounting for approximately 2-4 percent of births in developed countries like the US. ART outcomes depends heavily on the quality of the input materials (oocytes and sperm) used thus creating a growing need for better methods of sperm selection to select the most viable specimens with minimal damage.

ROS is the collective term that refers to the chemically reactive molecules containing oxygen, including the highly oxidative radicals such as hydroxyl radicals ($OH\cdot$), nonradical species such as the superoxide anion (O_2^-) or hydrogen peroxide (H_2O_2). This term can also refer to reactive nitrogen species (RNS), and both species are typical products of metabolism [25]. While low concentrations are required for many cellular processes, the levels are controlled by antioxidants. Some of these beneficial effects involve physiological roles, such as, defense against infectious agents, functions in cellular signaling pathways, and inducing a mitogenic response. In fact many ROS-mediated actions protect against ROS induced oxidative stress, maintaining a redox balance. In spermatozoa ROS are a required for a number of such purposes. For this reason they produce ROS themselves.

The principal type of ROS produced in spermatozoa is O_2^- which spontaneously produces H_2O_2 [26]. These ROS are typically not harmful to the spermatozoa due to the short half-lives and the antioxidant mechanisms present in order to maintain the key balance required for the ROS-related functions. These functions play a key role in capacitation, the series of events that occurs post ejaculation in the female genital tract to allow spermatozoa to fertilize the egg [27]. A fine balance of ROS and antioxidants are required for capacitation and ultimately fertilization. For example low levels of H_2O_2 are necessary for capacitation, but higher levels will reduce hyperactivation. This hyperactivation is the change in motility once in the female genital tract that allows interaction with the oocyte [28].

The proper balance of ROS and antioxidants are also required for eutherian mammalian chromatin compaction in maturing sperm. During the final stage of spermatogenesis histones are replaced by transitional proteins and then protamines, which will compact chromatin into toroid structures. Further compaction will take place when disulfide bonds are formed by the oxidation of thiol groups [29]. If packaging is abnormal then atypical morphology and infertility may occur.

Oxidative stress occurs when ROS levels become too high, or the antioxidant levels become too low. Highly oxidative ROS cause damage to cellular components, particularly to the DNA. Oxidative stress is the major source of damage to the DNA in spermatozoa. 8-Hydroxy-2-deoxyguanosine (8-OHdG), is an oxidized guanine base formed when DNA is damaged by the $OH\cdot$ radical, and is one of the major biomarkers in the detection of oxidative damage in DNA. Increased 8-OHdG concentration correlates with DNA fragmentation and strand breaks [30].

DNA repair is limited in spermatozoa, due to the high compaction of DNA in the nucleus. While this tight packaging may help protect DNA from further harm, it prevent DNA repair mechanisms from activating [31]. Therefore spermatozoa exposed to oxidative damage in the epididymis and during transport in the seminal fluid will accumulate damage with no opportunity to repair until it reaches the oocyte. DNA adducts caused by oxidative stress in sperm are thought to be repairable by the egg is the

damage is not extensive. Single and double stranded breaks to DNA not repaired lead to significant impacts of fertilization and pregnancy outcomes [32].

1. 3 Research motivation and introduction to specific projects

The work in this thesis is designed to principally address the potential of protamines, and other polycations, to provide protection of DNA in the packaged state from free radical damage. Our general hypothesis is that greater separation between DNA helices allows increased access to radical species resulting in more damaged nucleic acid bases. In Chapter 2, we will examine quantitatively if packaging DNA does provide protection from free radical damage. Our results show that not only is packaged DNA protected but that small differences in the packaging state can vary the capacity for free radical damage. In Chapter 3, we will focus on one proposed source of protamine dysfunction; the insufficient protamination in the sperm chromatin leading to defective sperm chromatin remodeling. Recent studies has shown that high rates of sperm DNA damage is not only related to infertility in men but also linked to higher rates of miscarriage as well as abnormal fetal development and higher rates of genetic disease in the offspring. Using reconstituted samples, we will examine underprotamination to provide quantitative insight into why protamine deficient nuclei are damaged.

CHAPTER 2: DNA DAMAGE IN PACKAGED AND UNPACKAGED DNA

2.1 Introduction

In this chapter, our focus is on determining quantitatively if packaging by polycations is able to protect DNA from damage by free radical species. As mentioned before, a major source of free radicals that could interact with the sperm cells are generated by the sperm cells themselves, as ·OH, often formed by a Haber-Weiss reaction or Fenton reaction. For our studies, we used three different systems to generate free radicals: AAPH [2,2'-Azobis(2-Amidinopropane) dihydrochloride], Copper(II) phenanthroline [$Cu(OP)_2$], and fenton reagents. The latter system is known to give ROS damage to DNA. The methods used to generate free radicals in these systems are described in the experimental section. Below, we first give some background into the mechanism for these different free radical sources.

The primary ROS generated in human spermatozoa is the O2•–. This one-electron reduction product of oxygen secondarily reacts with itself in a dismutation reaction, which is greatly accelerated by superoxide dismutase (SOD), to generate H2O2. In addition to H2O2 and O2•–, an array of secondary cytotoxic radicals and oxidants are generated by human spermatozoa. In the presence of transition metals, such as iron, H2O2 and O2•– can interact in a Haber-Weiss reaction to generate the extremely

pernicious hydroxyl radical (OH•) as in Figure 4.5 [16].

In addition, the hydroxyl radical can be produced by the Fenton reaction which requires a reducing agent such as ascorbate or ferrous ions

2.1.1 AAPH [2,2'-Azobis(2-Amidinopropane) Dihydrochloride]

AAPH [2,2'-Azobis(2-Amidinopropane) Dihydrochloride] is a free radical-generating azo compound [33]. One of the main advantages of using AAPH is its free radical generation can be easily controlled and measured. Although free radical generation can be slower compared to the other reagents used in this work, with heating AAPH can come to a steady state free radical concentration with heating. This ability of AAPH to come to steady state makes it an ideal model system and more reliable in producing the same amounts of damage between samples. Another advantage for this particular mode of action is that it can be frozen in a -20°C freezer after damaging, since the damaging reaction only takes place at 60°C. The combination of the slow reaction and high temperature allows for samples to be frozen, if desired, with no noticeable difference in the damage states when compared to an unfrozen sample.

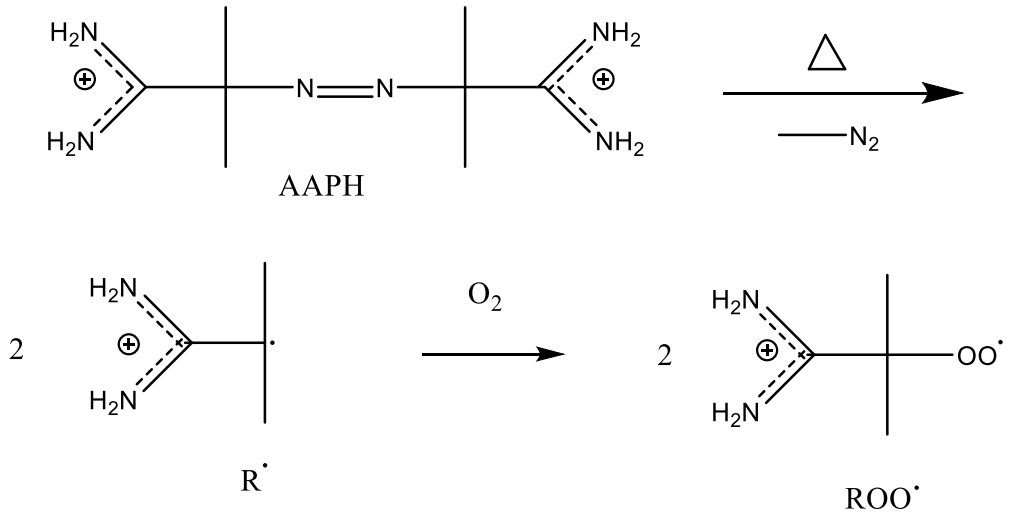

Figure 2.1 Degradation of AAPH mechanism.

Figure 2.1 shows the degradation mechanism of AAPH. After heat is applied the nitrogen molecule leaves and two $R^{\cdot}$ radicals are formed. Due to their instability, these two radicals rapidly combine with oxygen to form the $ROO^{\cdot}$ radical. This can Δ further degrade into $RO\cdot$ and $O_2^{\cdot -}$ which are the primary radicals that damage the DNA [34, 35].

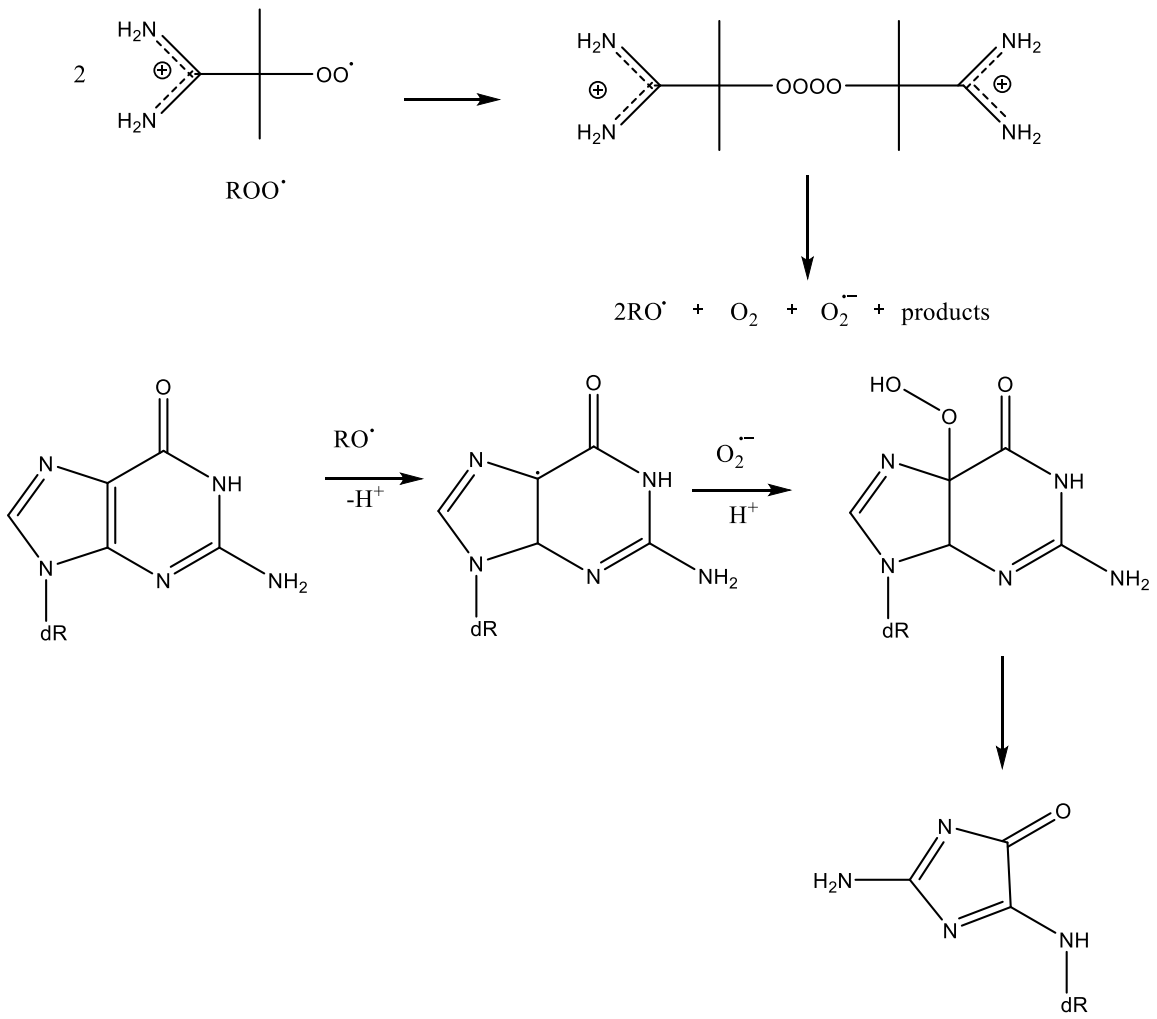

Figure 2.2 AAPH damage products.

Figure 2.2 depicts possible damage products formed from the AAPH. As one can see from the figure, there is no evidence of 8-oxo-dG damage from this system [36]. While this system does in fact damage DNA, as evident in our studies, the resulting damage is not an ideal model system for ROS damage since AAPH does not produce the common biomarker of oxidative stress observed in vivo. While instructive for basic studies, other damaging agents were also explored (copper phenanthroline and fenton reagent) to find systems more characteristic of ROS damage observed in natural sperm.

2.1.2 Copper-phenanthroline

Copper-phenanthroline, $Cu(OP)_2$, is one of many metal complexes that arbitrate DNA oxidation. $Cu(OP)_2$ is an example of a complex that damages DNA by radical processes. Due to its structure, as shown in Figure 2.3, $Cu(OP)_2$ is able to intercalate in the DNA complex. By intercalating into DNA, this allows the radicals generated by the copper to directly damage the DNA. The damage is seen in the way of single strand breaks at low concentration, and can fragment the DNA at higher concentration. This damage system works better than the other systems in our study at low concentration, and requires little time compared to that of AAPH.

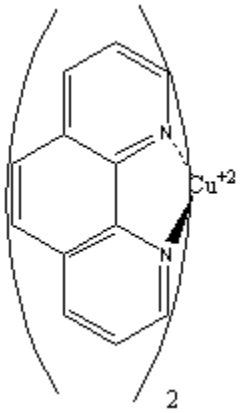

Figure 2.3 Structure of $Cu(OP)_2$

In the proposed mechanism depicted in Figure 2.4, the reaction starts when $Cu(OP)_2$ is mixed with a thiol reducing agent [37]. For our studies, dithiothreitol (DTT)

was used as the reducing agent. The reduced copper-phenanthroline is then able to react with hydrogen peroxide. The resultant copper-'oxo' compounds produce the observed DNA damage adducts.

$$2\ \mathrm{Cu^{II}(OP)_2} + 2\ \mathrm{RS^-} \rightarrow 2\ \mathrm{Cu^{I}(OP)_2} + \ \mathrm{RS-SR}$$

$$2\ \mathrm{Cu^{I}(OP)_2} + 2\mathrm{O_2} \rightarrow 2\mathrm{Cu^{II}(OP)_2} + 2\mathrm{O_2^{\cdot -}}$$

$$2\mathrm{O_2^{\cdot -}} + 2\mathrm{H^+} \rightarrow \mathrm{H_2O_2} + \mathrm{O_2}$$

$$\mathrm{Cu^{I}(OP)_2} + \mathrm{H_2O_2} \rightarrow \mathrm{Cu(OP)_2 - "oxo"}$$

$$\mathrm{Cu^{I}(OP)_2 - "oxo" + DNA} \rightarrow \mathrm{Cu^{II}(OP)_2 + DNA\ damage}$$

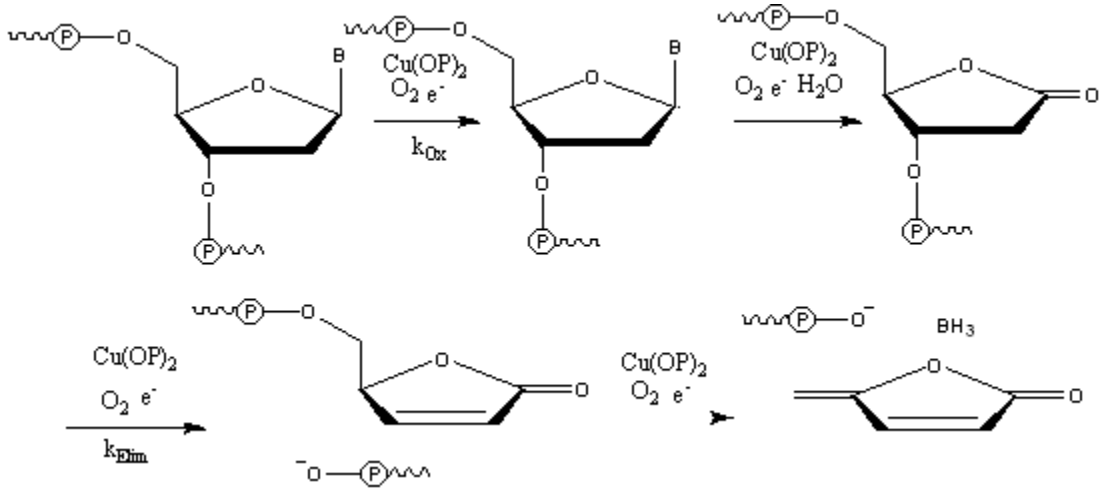

Figure 2.4 Mechanism for DNA damage and single strand break by $Cu(OP)_2$.

2.1.3 Fenton

One of the most well known radical generators is the Fenton reaction. The Fenton reagent occurs with just Iron(II) and hydrogen peroxide and produces two separate oxygen-radical species.

$$Fe^{2+} + H_2O_2 \rightarrow Fe^{3+} + HO\cdot + OH^-$$

$$Fe^{3+} + H_2O_2 \rightarrow Fe^{2+} + HOO\cdot + H^+$$

These radical species are able to go on to damage DNA by forming base adducts. The damage is similar to that of $Cu(OP)_2$ but less localized on the DNA strands, these radicals occur throughout the solutions. Unlike $Cu(OP)_2$, standard fenton reagents do not intercalate within DNA.

2.2 Methods and materials

The following methods were used for the studies discussed in this chapter of the thesis to investigate oxidative damage in the packaged and unpackaged DNA.

2.2.1 Materials

2,2'Azobis(2-amidinopropane) dihydrochloride (AAPH), Ethidium bromide (EtBr), and Dithiothreitol (DTT) were purchased from Acros organics (Geel, Belgium). 200 proof Ethanol, puc19 plasmid DNA, EcoR1 restriction enzyme, and 10X NE buffer were purchased from New England Biolabs (Ipswich, MA). 10X Phosphate buffer was purchased from Fisher Scientific (Waltham, MA). 30% w/w Hydrogen peroxide, Iron(II) sulfate heptahydrate [$Fe(II)SO_4$], Protamine chloride from salmon (grade V histone free), Sodium azide (NaN_3), and Dextran Sulfate (DS) sodium salt were purchased from Sigma-Aldrich (St. Louis, MO). TAE buffer was purchased from Omega biotek (Norcross, GA). 3M sodium acetate was purchased from teknova (Hollister, CA). 1M Tris buffer was purchased from cellgro (Tewksbury, MA). K6 and R6 were purchased from GeneScript. 1,10 copper phenanthroline $Cu(OP)n_2$ was received from Dr. Phoebe Glazer.

2.2.2 AAPH damage treatment

To treat sample with AAPH [2,2'Azobis(2-amidinopropane) dihydrochloride], the following steps were followed. AAPH was dissolved in de-ionized water. The resultant AAPH solution was heated to 60°C for 1 hr to help the free radical concentration achieve a steady state. While the AAPH solution was heating, DNA, de-ionized water, and phosphate buffer were mixed. Phosphate buffer final concentration in the reaction was

11.9 mM, pH 7.4. Upon completion of the 1 hr pre-incubation, AAPH was added to the DNA buffer solution bringing the total reaction volume up to 15μL. 400 ng of puc 19 plasmid DNA was used for each sample to provide sufficient DNA for gel electrophoresis. The solution of DNA and AAPH was allowed another 1hr to incubate. After this time, the damaged DNA samples were frozen in a -20°C freezer. On the following day, the samples were thawed and mixed with 2 μL 6X loading buffer. The 17 μL of solution were then loaded into the appropriate lanes on a 0.8% Agarose gel. Gel electrophoresis was conducted with 10 V/cm being applied to the gel. This was allowed to run in 600mL of 1x TAE buffer. After 120 minutes, gels were stained for one hour in 2.5 μg/mL ethidium bromide/1x TAE staining solution on a shaker. Gels were then destained in 1x TAE buffer for 30 minutes before imaging.

2.2.3 AAPH damage treatment with condensing agent

To treat condensed samples with AAPH, the following steps were followed. AAPH was dissolved in de-ionized water. The resultant solution was left to pre-incubate for 1 hr at 60°C. While the AAPH solution was left to warm the DNA, de-ionized water, condensing agent and phosphate buffer were mixed, and the DNA/condensing agent were allowed to condense a minimum of 15 minutes. Phosphate buffer final concentration in the reaction was 11.9 mM, pH 7.4. Upon completion of the 1 hr pre-incubation, the AAPH was added to the polycation-DNA solution to bring the total reaction volume up to 15 μL. The DNA used each time was 400 nanograms of puc19 plasmid. The mixed

solutions were then allowed to incubate for 1 hr. After this time had passed the samples were frozen in a -20°C freezer. On the following day the samples were mixed with 2 µL 6X loading buffer and 2 µL of 15 µg/µL decondensing agent, dextran sulfate [38]. The 19 µL of solution were then loaded into the appropriate lanes on a 0.8% Agarose gel. Gel electrophoresis was conducted with 10 V/cm being applied to the gel. This was allowed to run in 600mL of 1x TAE buffer. After 120 minutes the gel was stained in 2.5 µg/mL ethidium bromide/1x TAE for one hour on a shaker. Destain time was ½ hour in 1xTAE. Image was then taken under UV light

2.2.4 $Cu(OP)_2$ damage treatment

To treat with copper 1,10-phenanthroline $Cu(OP)_2$ the following steps were taken. 400 nanograms of puc19 plasmid DNA were mixed with phosphate buffer, de-ionized water, and $Cu(OP)_2$. Phosphate buffer final concentration in the reaction was 11.9mM, pH 7.4. The volume of water and final concentration of $Cu(OP)_2$ were modified to achieve the desired free radical concentrations. Along the sides of the reaction vessel, two separate volumes of dithiothreitol (DTT) and hydrogen peroxide (H_2O_2) were pipetted, but not mixed with the DNA solution, so the final concentration of both DTT and H_2O_2 would be 1mM. The reaction vessels were then centrifuged allowing for simultaneous mixing of DTT, H_2O_2 and the DNA solution in all the tubes. The final volume was maintained constant in all samples at 15 µL. Reaction was incubated at room temperature for 30 minutes. Immediately following the reaction, 2 µL of 6x loading buffer were

mixed in with the sample and the full reaction volume was loaded into a 0.8% Agarose gel. Gel electrophoresis was conducted at an applied voltage of 10 V/cm and run for approximately 2 hours in 600 mL of 1x TAE buffer. Gels were then stained in 200 mL 2.5 μg/mL ethidium bromide/1x TAE staining solution for one hour with shaking then destained for 30 mins in an equal volume of 1x TAE destaining solution before imaging.

2.2.5 $Cu(OP)_2$ damage treatment with condensing agent

To treat condensed samples with $Cu(OP)_2$ the following steps were taken. 400 nanograms of puc19 plasmid DNA was mixed with phosphate buffer, de-ionized water, condensing agent and $Cu(OP)_2$. The final phosphate buffer concentration in the reaction was 11.9mM, pH 7.4. This solution was allowed to remain undisturbed for a minimum of 15 minutes. The volume of water and the final concentration of $Cu(OP)_2$ was changed to achieve the desired concentrations for the experiment. Along the sides of the reaction vessel, two separate volumes of DTT and H_2O_2 were pipetted, but not mixed with the DNA solution, so the final concentration of both DTT and H_2O_2 would be 1mM. The reaction vessels were then centrifuged allowing for simultaneous mixing of DTT, H_2O_2 and the DNA solution in all the tubes. The final volume was maintained constant in all samples at 15 μL. Reaction was incubated at room temperature for 30 minutes. Immediately following the reaction, 2 μL of 6x loading buffer and 2 μL of decondensing agent (dextran sulfate, DS) were mixed in with the sample and the full reaction volume was loaded into a 0.8% Agarose gel. Gel electrophoresis was conducted at an applied

voltage of 10 V/cm and run for approximately 2 hours in 600 mL of 1x TAE buffer. Gels were then stained in 2.5 μg/mL ethidium bromide/1x TAE staining solution for one hour with shaking then destained for 30 mins in an equal volume of 1x TAE destaining solution before imaging.

2.2.6 Fenton damage treatment

To treat with fenton reagent, the following steps were taken. Iron(II) sulfate, phosphate buffer, de-ionized water, and puc19 plasmid DNA were mixed together. Final concentration of phosphate was 11.9mM, pH 7.4. The volume of iron and water added was varied to achieve the desired concentration. H_2O_2 was added along the side wall of the reaction vessel, so that final concentration would be 1mM. The final reaction volume was 15 μL Reaction vessels were subsequently centrifuged allowing the H_2O_2 solution to mix with the DNA solution simultaneously for all reactions. The Fenton reaction was incubated for 30 mins at room temperature. Immediately following reaction, 2μL of 6x loading buffer was mixed with the sample. The resultant 17μL of solution was loaded on to a 0.8% Agarose gel. Gel electrophoresis was conducted at an applied voltage of 10 V/cm and run for approximately 2 hours in 600 mL of 1x TAE buffer. Gels were then stained in 2.5 μg/mL ethidium bromide/1x TAE staining solution for one hour with shaking then destained for 30 mins in an equal volume of 1x TAE destaining solution before imaging.

2.2.7 Fenton damage treatment with condensing agent

To treat condensed sample with fenton reagent, the following steps were taken. Iron(II) sulfate, phosphate buffer, de-ionized water, condensing agent and puc19 plasmid DNA were mixed together. The final concentration of phosphate was 11.9mM, pH 7.4. The concentration of iron and water were varied to achieve the desired iron concentrations. The final reaction volume was 15μL. This solution was allowed to condense for a minimum of 15 minutes. Sufficient H_2O_2 was added along the side wall of the reaction vessel to achieve a final H_2O_2 concentration of 1mM. The final reaction volume was 15μL. Reaction vessels were subsequently centrifuged allowing the H_2O_2 solution to mix with the DNA solution simultaneously for all reactions. The Fenton reaction was incubated for 30 mins at room temperature. Immediately following reaction, 2μL of 6x loading buffer and 2 μL of decondensing agent, dextran sulfate, were mixed with the sample. The resultant 19 μL of solution was loaded on to a 0.8% Agarose gel. Gel electrophoresis was conducted at an applied voltage of 10 V/cm and run for approximately 2 hours in 600 mL of 1x TAE buffer. Gels were then stained in 2.5 μg/mL ethidium bromide/1x TAE staining solution for one hour with shaking then destained for 30 mins in an equal volume of 1x TAE destaining solution before imaging.

2.2.8 EcoR1 Digestion

For determination of linear DNA bands compared to supercoiled and open coiled plasmid bands by gel electrophoresis, puc19 plasmid DNA was linearized using EcoR1 enzyme purchased from New England BioLabs (NEB) following provided protocols. Briefly, plasmid DNA, EcoR1, de-ionized water and 10 μL of reaction Buffer were mixed together into one solution. The solution was then incubated on a heat block at 37°C for fifteen minutes. The linearized DNA was purified by ethanol precipitation and subsequently stored at -20°C until required.

2.2.9 Ethanol Precipitation

To separate our digested DNA plasmid from enzyme, an ethanol precipitation was performed. 0.3M sodium acetate and three times the DNA sample volume of cold (-20°C) ~99% ethanol were mixed and placed overnight at -20°C. The following day the solution was spun at 15000 x g for 20 minutes. Supernatant was subsequently removed and disposed. 400 μL of 70% cold (-20°C) Ethanol was then added to the pellet and mixed. Samples were then centrifuged for 10 mins at 15000 x g and the supernatant was removed and the samples dried in a centrivap. The dried DNA pellet was resuspended in a TE buffer with 400 μM NaN_3 and stored at -20°C.

2.3 Characterization Techniques

The primary investigative technique employed to examine DNA damage in the packaged and unpackaged state was gel electrophoresis. The following section will cover the details of how this technique was employed.

2.3.1 Gel Electrophoresis

All gel images were taken after a staining/destaining procedure. Gels were cast in a 9 X 11 cm plastic plate with a comb dividing the gel into ten lanes. Each gel was made in a 0.8% agarose solution, buffered with 1x TAE. Running buffer solution was composed of 1X TAE solution. Current was applied to the gel with a FB300 power supply, purchased from Fischer Scientific. Gels were run for approximately two hours, and then stained for one hour in 2.5 μg/mL EtBr for visualization. After gels were destained in 1X TAE buffer for 30 minutes gel images were recorded in an image box under Ultra-violet light with an ethidium bromide filter.

2.3.2 Gel Electrophoresis theory

Agarose gel electrophoresis is one of the most common ways of separating DNA base fragments. In this technique DNA is pulled through an agarose gel by an electric field and the resultant fragments are separated by their size and shape [39]. Agarose is composed of repeated agarobiose (L- and D-galactose) subunits [40]. In the gelation process these agarose polymers will combine non-covalently after subsequent heating and cooling. These polymers will form pores through which the DNA will move. The concentration of the agarose will determine the overall size of the pores, with a higher concentration correlating to a smaller pore [41]. After the agarose gel has set, running buffer is poured over the gel to allow conduction of uniform current. Loading buffer if mixed with a dye to enable the sample of interest to sink into the gel as well as track how far the DNA has traveled.

Once the gel is prepared, DNA can be successfully separated due to the negatively charged phosphate backbone on DNA. When an electric field is applied in the gel, DNA will move towards the positively charged anode. The rate at which this takes places is contingent on the size of DNA, the agarose concentration, DNA conformation, and voltage applied [39]. After the gel has finished running, the gel is stained with EtBr to allow visualization of the DNA. When EtBr is exposed to ultraviolet light, electrons in the aromatic ring of the ethidium molecule are excited to a higher energy state. After they relax to their ground state excess energy is given off in the form of light as they return to

their ground state [39]. EtBr is also able to intercalate into the DNA molecule in a predictable manner. So by this the intensity of the DNA band can predict its concentration [42].

2.4 Results and Discussion

Fig 2.5 shows DNA bands observed by gel electrophoresis in the unpackaged state, packaged state as well as subsequent release from the packaging state. In the leftmost lane in figure 2.5, puc19 plasmid DNA was run as received. Two bands are observed, the lower dominant band corresponds to supercoiled DNA. This supercoiled (SC) DNA is the result of highly twisted DNA strands [43-45]. In most organisms, such as the plasmid used in this study, the DNA is negatively supercoiled [46]. Due to the compaction of the DNA in the supercoiled state, the supercoiled DNA is able to move through the gel matrix more quickly. Open coil (OC) DNA is the result of DNA being nicked, or damage in some way. Once nicked, the tension on the DNA is relieved and the DNA reverts back to its relaxed state. Since this is a DNA plasmid, the relaxed state is an open coil that moves much slower through the gel matrix. A faint band is observed from the untreated puc19 showing a small fraction of open coiled plasmid is present in the commercial product as received. Linear DNA would result from a double strand break of a plasmid. Linear DNA is able to move faster through the gel than an open coil, but slower than the highly packaged supercoiled DNA. Using EcoRI, we have determined approximately where the linear band runs and this is indicated in Figure 2.5.

The second lane in figure 2.5 shows the result of DNA condensation by protamine. No bands are observed in the region of interest. The DNA-protamine complex is not able to move through the gel due to the large complex size as well as the charge neutralization of the DNA phosphates in the condensed state. With no negative charge, the DNA would not be drawn to the positive charge at the opposite end of the gel. Typically with fully condensed polycation-DNA complexes, either no fluorescence is observed or some sample is observed in the sample wells that were unable to diffuse into the gel matrix. Here the protamine-DNA complex was made at a nitrogen to phosphate (N:P) charge ratio of 2 resulting in fully condensed DNA.

Next we wanted to establish that condensed DNA could subsequently be released from the complex using a polyanionic competitor, here dextran sulfate (DS), and that the packaging/unpackaging process does not damage the DNA. Dextran sulfate was chosen as a competing agent for the protamine due to its high number of negative charges in which to bind the positively charged residues, encouraging protamine release from DNA. Dextran sulfate was also readily available and inexpensive in comparison to heparin, another commonly agent used to bind protamine. The right side of Figure 2.5 shows protamine-DNA complexes (N:P 2.0) competed against increasing amounts of DS. 10μg of dextran sulfate (DS) is sufficient to release the protamine without affecting the motility of the bands. At 2μg DS it appears the DNA band is shifted up, indicating that this is not enough to fully release the DNA. These studies not only confirmed DNA release by competition with DS but also no nicking is observed with the relative ratios of SC to OC being constant.

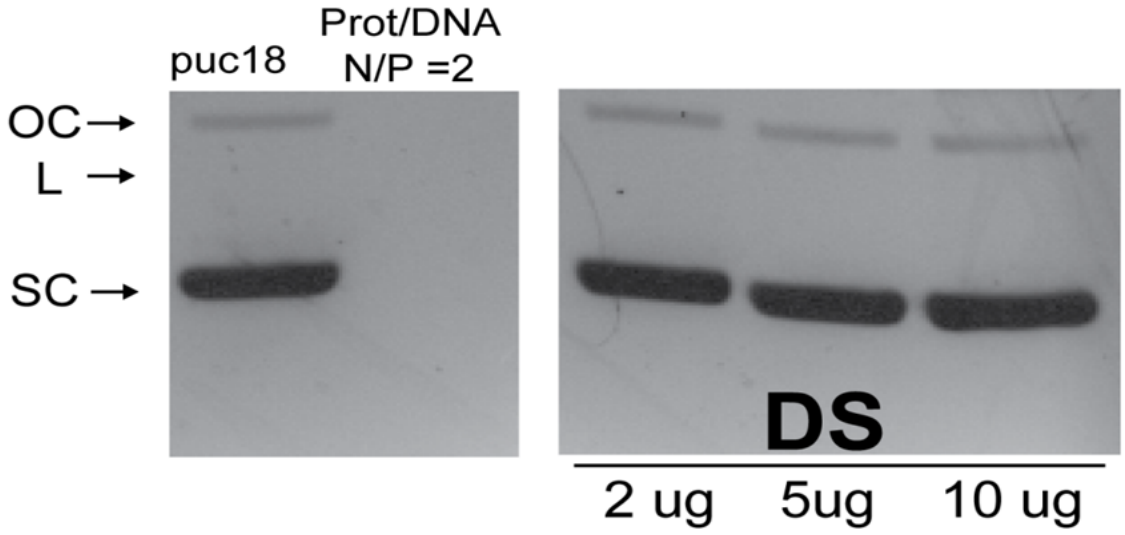

Figure 2.5 Protamine induced condensation of DNA and release. (left) Gel electrophoresis of unpackaged and protamine packaged puc19 plasmid DNA. The location of supercoiled (SC), open coiled (OC) and linear plasmid is indicated (right) Release of DNA from protamine-DNA (N:P 2) complexes with increasing dextran sulfate (DS) concentration.

2.4.1 AAPH damage studies

The first DNA damage studies performed focused on AAPH (2,2'Azobis (2-amidinopropane) dihydrochloride) as the free radical source. Initial work focused on establishing the concentration of AAPH required to damage DNA. Figure 2.6 shows puc19 plasmid DNA damage as a function of increasing AAPH concentration. With increasing AAPH concentration, a shift is observed with an increase in the observed open coil band at the expense of the supercoiled band.

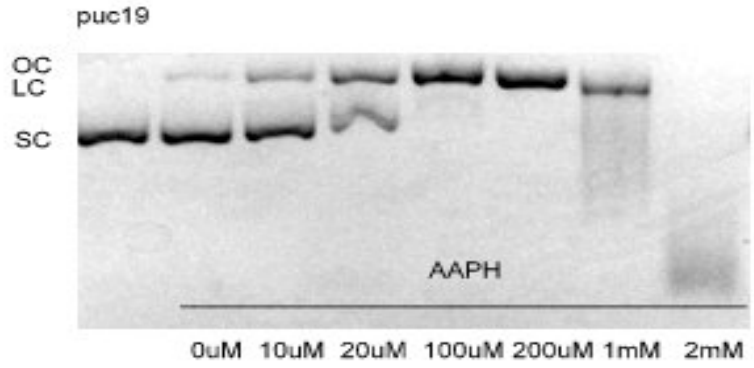

Figure 2.6 DNA damage by AAPH. Lane 1 - 400ng of untreated puc19 plasmid; Lane 2 DNA heated to 60°C without AAPH for 1 hour; Lane 3 to 8 – DNA treated with increasing AAPH concentration and incubated for 1 hour at 60°C.

This suggests these concentrations of AAPH are sufficient to nick the supercoiled plasmid. At still higher AAPH concentrations linear DNA bands or smearing, resulting from highly digested DNA of various molecular weights, are observed. At ~2mM AAPH, we see the plasmid is nearly fully digested.

Next we want to simply ask if we can use gel electrophoresis to observe quantitatively the protection afforded DNA by packaging by protamine. Figure 2.7 shows the effect of packaged DNA vs unpackaged DNA at varying concentrations of AAPH. As expected, DNA packaged by protamine is more protected from AAPH induced radicals, when compared to the adjacent damaged DNA. In lane 2, we show untreated puc19 plasmid DNA is nearly completely in the supercoiled state. Lane 3 shows protamine at

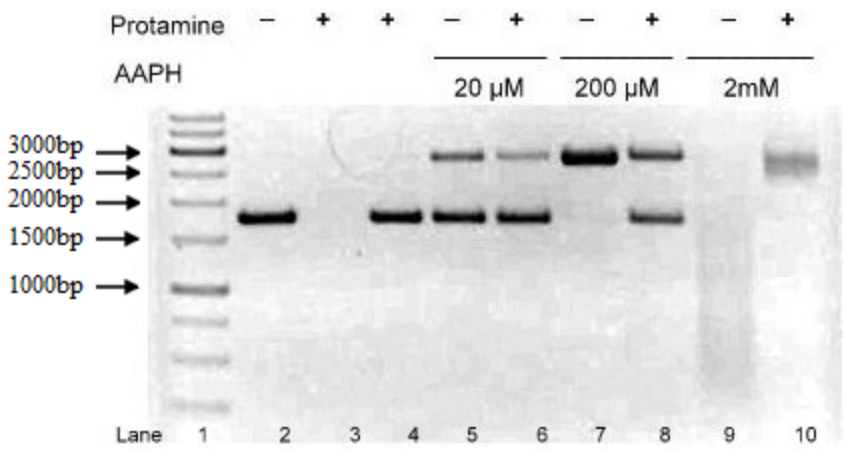

Figure 2.7 Packaged and unpackaged DNA's susceptibility to damage induced by AAPH. Lane 1 – 400 ng of 1kb ladder; Lane 2 - 400ng of puc19 plasmid DNA; Lane 3 - DNA condensed with protamine, N:P 2.0; Lane 4 – DNA condensed with protamine N:P 2.0, released with 30µg of dextran sulfate; Lane 5 - DNA packaged treated with 20µM AAPH Lane 6 - DNA packaged with protamine N:P 2.0 treated with 20µM AAPH; Lane 7 - DNA treated with 200µM AAPH; Lane 8 - DNA packaged with protamine N:P 2.0 treated with 200µM AAPH; Lane 9 - DNA treated with 2mM AAPH; Lane 10 – DNA packaged with protamine N:P 2.0 treated with 2mM AAPH.

N:P 2 is sufficient to complete complex the DNA. Lane 4 shows that the packaged DNA can be fully released with sufficient dextran sulfate competitor. Lanes 5 to 10 show side by side comparisons of naked DNA and packaged DNA damage at increasing AAPH concentrations. At 20µM AAPH, unpackaged DNA appears to be half open coil form and half supercoiled form due to single strand breaks occurring with exposure to the free radical. Protamine condensed DNA, in contrast, is still about 85% in the supercoiled state. 200µM AAPH is sufficient to completely nick the unpackaged DNA (lane 7) resulting in no supercoiled band being observed. Once packaged with protamine the plasmid is again afforded a good deal of protection. Protamine packaged DNA (lane 8) at

the same concentration still maintains about half the DNA in the supercoiled state. At very high AAPH concentration (2 mM), naked DNA (lane 9) is completely digested while packaged DNA (lane 10) is able to maintain much of the sample in the open coil or linear state as evident by discrete bands being observed by gel electrophoresis.

Next we wanted to examine if subtle changes in the packaging state has an effect on the protection of DNA from AAPH damage. Such subtle changes would presumably be more consistent with possible mispackaging occurring in vivo during defective sperm chromatin remodeling. Here, protamine-DNA was compared to unpackaged DNA as well as DNA packaging by R6 and K6 peptides. These two peptides were selected because the DNA spacing after packaging by the peptides was published in an earlier study [47]. The interaxial DNA-DNA spacing (D_{int}) observed for the hexagonally packaged DNA condensed by K6-DNA was reported as 32.3 Å, salmon protamine-DNA 29.3 Å, and R6-DNA 28.6 Å. All were reported with a resolution of ± 0.1 Å. Figure 2.8 is included to show that hexalysine and hexaarginine condense DNA similarly to protamine. At N:P 1.0 most of the DNA is bound to the various condensing agents, but at N:P 2.0 all the DNA is bound by the condensing agents. The length of the gel is included to show evidence of some complex sticking in the wells (lanes 4, 7, & 9). These faint bands are evidence that the DNA/protamine complex is not pulled through the matrix. This is likely a combination of the complex being too large to move through the matrix, and lacking a negative charge therefore not being attracted to the positive electrode at the opposite end of the gel.

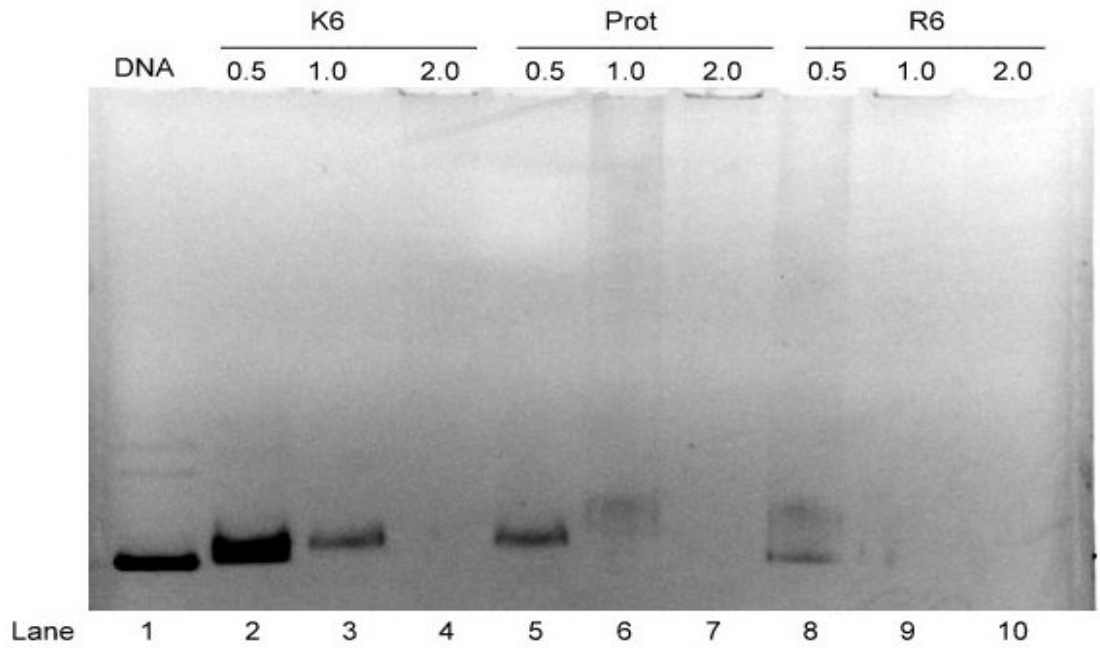

Figure 2.8 Condensation of DNA by K6, protamine, and R6. Lane 1 – 400ng of puc19 plasmid. Lane 2 – DNA condensed by K6 (N:P 0.5). Lane 3 – DNA condensed by K6 (N:P 1.0). Lane 4 – DNA condensed by K6 (N:P 2.0). Lane 5 – DNA condensed by Protamine (N:P 0.5). Lane 6 – DNA condensed by Protamine (N:P 1.0). Lane 7 – DNA condensed by Protamine (N:P 2.0). Lane 8 – DNA condensed by R6 (N:P 0.5). Lane 9 – DNA condensed by R6 (N:P 1.0). Lane 10 – DNA condensed by R6 (N:P 2.0).

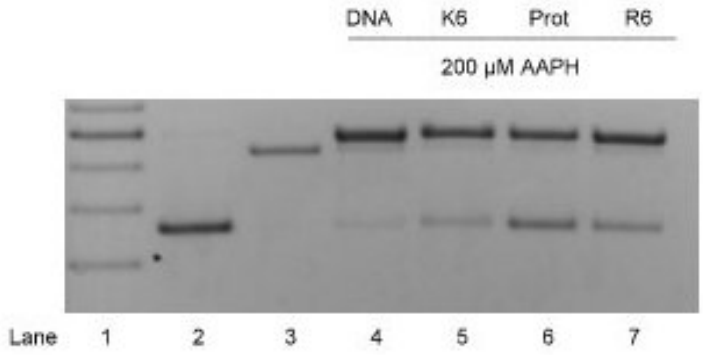

Figure 2.9 Various packaging states susceptibility to AAPH. Lane 1 – 1kb Ladder; Lane 2 – 400ng Puc19 plasmid DNA; Lane 3 – EcoR1 linearized DNA; Lane 4 – DNA treated with 200μM AAPH; Lane 5 – DNA packaged with K6 (N:P 2) treated with 200μM AAPH; Lane 6 – DNA packaged with protamine (N:P 2) treated with 200μM AAPH; Lane 7 – DNA packaged with R6 (N:P 2) treated with 200μM AAPH

Figure 2.9 shows all these samples treated with 200μM AAPH and the damage that accrued was compared to the DNA in variously packaged states. The distinction between linearized DNA and open coil can confidently be stated with the inclusion of the EcoR1 linearized DNA in lane 3. This inclusion allows differentiation between the linear band and open coil band. All packaged DNA samples were made at the same N:P 2 charge ratio sufficient for complete DNA condensation for all three peptides. 200μM AAPH was sufficient to fully damage the DNA resulting in a near complete loss of the super coiled band with the entire DNA being observed in either the open coiled or linear bands (lane 4, Fig 2.9). The more openly packaged K6-DNA complex resulted in only marginal protection at this AAPH concentration. The similar packaging density systems, protamine-DNA and R6-DNA provide more protection than K6 as evidenced by the increased supercoiled band.

2.4.2 $Cu(OP)_2$ Damage Studies

So as to not rely on only one free radical system, we also looked at DNA damage in the packaged and unpackaged state using other free radical systems. The next system used to damage DNA was copper (II) 1,10 phenanthroline, $Cu(OP)_2$. A unique feature of $Cu(OP)_2$ is its ability to intercalate into the DNA and actively cause DNA damage generally attributed to a copper-oxo species as discussed in section 2.1.2 resulting primarily in multiple single-strand breaks of DNA. This unique interaction of copper phenanthroline with DNA creates copper-oxo species capable of damaging DNA at particularly high concentrations directly in the vicinity of the DNA bases. We hypothesize therefore that the degree of protection afforded by packaged DNA to $Cu(OP)_2$ may be diminished.

Figure 2.10 shows damage on unpackaged puc19 plasmid DNA as a function of $Cu(OP)_2$ concentration. Lane 2 shows untreated puc19 plasmid with nearly all the DNA in the supercoiled state. With as low as 10 μM $Cu(OP)_2$, nearly all the supercoiled DNA is nicked resulting in a shift in the gel electrophoresis to the open coiled state. With increasing $Cu(OP)_2$ concentration, we see more damage accruing resulting in all the DNA being in the open coiled state (lane 4) and even possibly double strand breaks of the DNA by 50 μM. At this concentration, initial signs of fragmentation appear with the presence of smearing in the gel. For comparison, lane 8 contains 400ng of EcoR1 linearized DNA. By 75 μM $Cu(OP)_2$ the plasmid is completely fragmented resulting in no observed bands by gel electrophoresis. We have observed some variance from gel to gel on the damage

observed for a given $Cu(OP)_2$ concentration; however the general trend of more damage with increasing $Cu(OP)_2$ concentration holds. Interestingly, at 50μM $Cu(OP)_2$, we often observed a linearization of the plasmid DNA comparable to that achieved with EcoRI enzyme.

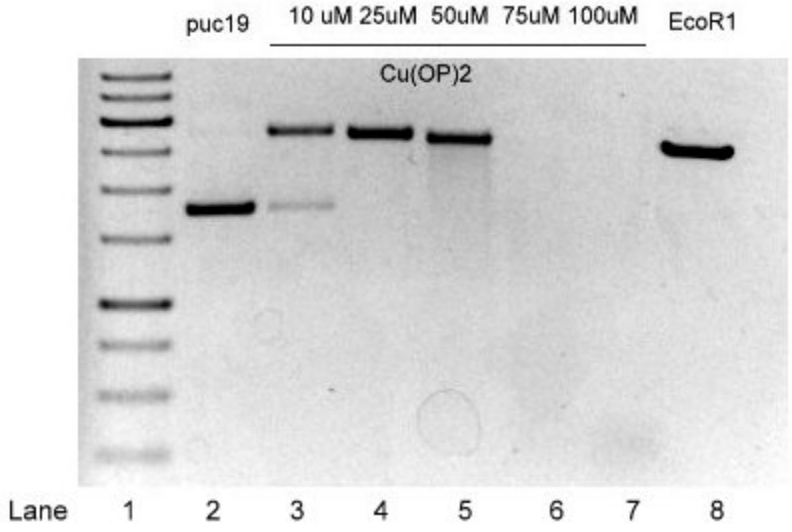

Figure 2.10 $Cu(OP)_2$ damage assay. Lane 1 – 400ng of 1kb ladder; Lane 2 – 400ng of puc19 plasmid DNA; Lane 3 – DNA treated with 10μM $Cu(OP)_2$; Lane 4 – DNA treated with 25μM $Cu(OP)_2$; Lane 5 – DNA treated with 50μM $Cu(OP)_2$; Lane 6 – DNA treated with 75μM $Cu(OP)_2$;Lane 7 – DNA treated with 100μM $Cu(OP)_2$; Lane 8 – EcoR1 linearized DNA.

Next we examined the ability of protamine to protect DNA from $Cu(OP)_2$ initiated damage at different concentrations. As shown in figure 2.11, similar to its ability to protect DNA from AAPH, protamine-DNA is sufficiently packaged to protect it from $Cu(OP)_2$. At 10μM $Cu(OP)_2$ unpackaged DNA is approximately 50% supercoiled and

50% open coil DNA. Once packaged at N:P 2.0 with protamine, the majority of the DNA remains in the supercoiled phase. At 50μM $Cu(OP)_2$, unpackaged DNA appears to be

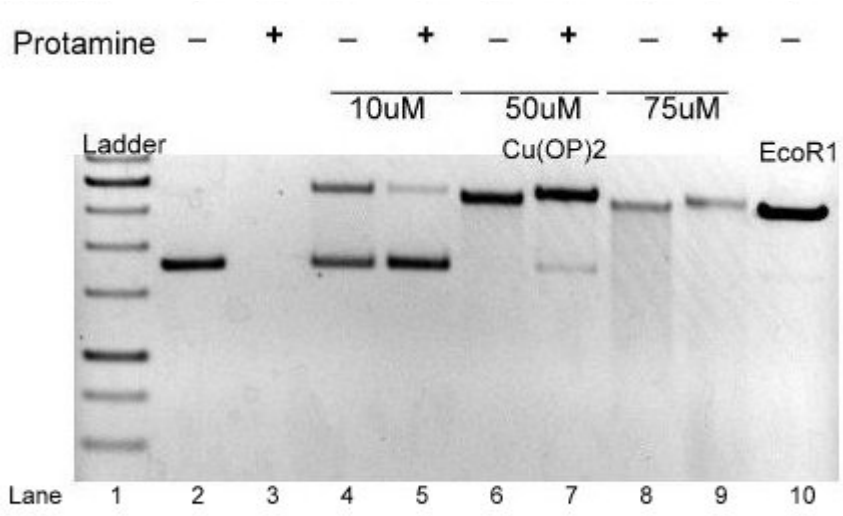

Figure 2.11 Packaged and unpackaged DNA's susceptibility to damage induced by $Cu(OP)_2$. Lane 1 – 400ng of 1kb ladder; Lane 2 - 400ng of puc19 plasmid DNA; Lane 3 DNA condensed with protamine (N:P 2.0); Lane 4 - DNA treated with 10μM $Cu(OP)_2$; Lane 5 - DNA packaged with protamine treated with 10μM $Cu(OP)_2$; Lane 6 - DNA treated with 50μM $Cu(OP)_2$; Lane 7 - DNA packaged with protamine treated with 50μM $Cu(OP)_2$; Lane 8 - DNA treated with 75μM $Cu(OP)_2$; Lane 9 – DNA packaged with protamine treated with75μM $Cu(OP)_2$; Lane 10 - EcoR1 linearized DNA.

linearized with some fragmentation. Protamine condensed DNA, however shows a slight supercoiled band with the remainder of the DNA in the open coiled state. At high $Cu(OP)_2$ concentration, the packaged state is only slight more protected than the unpackaged state.

Next we examined the effects of different packaging densities on the ability of the polycation-DNA complex to protect DNA from $Cu(OP)_2$. As discussed earlier, arginines

can condense DNA to much tighter packaging densities compared to comparable lysine condensing agents. Hexapeptides of arginine and lysine have a difference of ~ 3.7 Å in the resulting DNA-DNA spacings observed in the condensed state. Protamine-DNA packaging is slightly less than R6-DNA. Figure 2.12 shows the results of various packaging states susceptibility to $Cu(OP)_2$. At 50μM $Cu(OP)_2$, the DNA is linearized with a sizeable portion fragmented as evident by the observed smearing in the gel. EcoRI

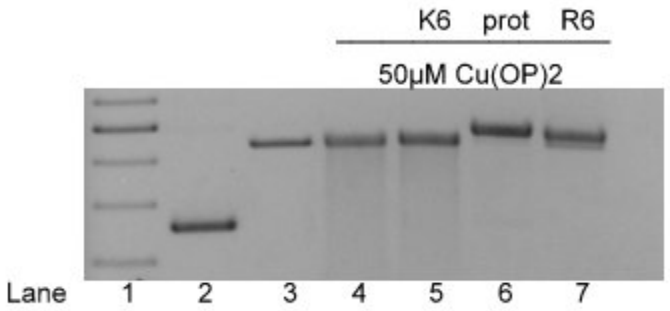

Figure 2.12 Various packaging states susceptibility to $Cu(OP)_2$. Lane 1 – 400ng of 1kb Ladder; Lane 2 – 400ng Puc19 plasmid DNA; Lane 3 – EcoR1 linearized DNA; Lane 4 – DNA treated with 50μM $Cu(OP)_2$; Lane 5 – DNA packaged with K6 (N:P 2.0) treated with 50μM $Cu(OP)_2$; Lane 6 – DNA packaged with protamine (N:P 2.0) treated with 50μM $Cu(OP)_2$; Lane 7 – DNA packaged with R6 (N:P 2.0) treated with 50μM $Cu(OP)_2$.

linearized DNA is shown in lane 3 for comparison with the unpackaged DNA treated with $Cu(OP)_2$ (lane 4). When packaged with K6 at N:P 2, the DNA does not seem to be significantly protected beyond unpackaged DNA. Changing the DNA packaging by just a few angstroms however improves the protection from 50μM $Cu(OP)_2$ as evidenced by

salmon protamine and R6 packaged DNA both condensed at N:P 2. Lane 6 and lane 7 show the elimination of the DNA fragmentation and bands consistent with DNA in the open coiled state. Interestingly while R6 is slightly more tightly packaged compared to protamine there seems to be some evidence for double strand breaks in this sample. In theory the smaller the space between the DNA, the less access damaging agents will have to the DNA. This may be the result of the variation between samples in the free radical concentration or indicative that other factors may be at play for the protective capacity of protamine over pure arginine peptides. More advanced methods may need to be performed in order to more accurately define what role the spacing of DNA has to play.

2.4.3 Fenton damage studies

The last free radical system studied was Fenton reagent; a solution of hydrogen peroxide with ferrous (Fe^{2+}) iron as a catalyst. Fenton reagent is often used for biological studies and believed to create damage comparable to ROS in vivo. While AAPH and $Cu(OP)_2$ don't damage by directly producing biological like ROS, the fenton reaction does. In this way, fenton reagent could give us a better approximation to damage occurring in vivo. Figure 2.13 shows unpackaged puc19 plasmid DNA damage as a function of increasing fenton concentration. Consistent with all the previous gels, all samples consist of 400 ng plasmid DNA per well. DNA is observed to damage in a systematic way with increasing iron concentration and fixed H_2O_2 concentration. At the lowest concentration shown, 0.5mM Fe(II), about half of the DNA present was damaged

to an open coil state and the remaining half was undamaged in the supercoiled state. By 1mM Fe(II), the DNA is primarily open coil with small amount damaged enough to the linear band. Increasing to 2mM Fe(II) concentration, shows a systematic rise in the linear

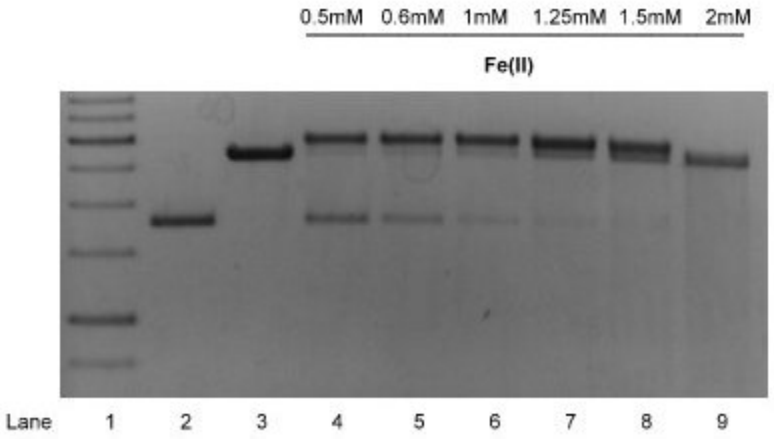

Figure 2.13 DNA damage by induced Fenton reaction. Lane 1 – 400ng of 1kb ladder; Lane 2 – 400ng of puc19 plasmid DNA; Lane 3 – EcoR1 linearized DNA; Lane 4 – DNA treated with 0.5mM fenton reagent; Lane 5 – DNA treated with 0.6mM fenton reagent; Lane 6 – DNA treated with 1mM fenton reagent; Lane 7 – DNA treated with 1.25mM fenton reagent; Lane 8 – DNA treated with 1.5 mM fenton reagent; Lane 9 – DNA treated with 2mM fenton reagent.

DNA band at the expense of the open coil band as well as increased smearing representing DNA fragmentation. For reference, EcoRI linearized DNA is shown in lane 3.

Next we examined the ability of protamine-DNA (N:P 2) to protect DNA from damage by Fenton reagent. Figure 2.14 shows that significant protection from oxidative

damage occurs for protamine-DNA compared to unpackaged DNA consistent with the previous damage studies using AAPH and $Cu(OP)_2$. Lane 1-4 show various controls of a 1kbp ladder, untreated puc19 plasmid DNA primarily in the supercoiled state, fully packaged protamine-DNA (N:P 2), and EcoRI linearized DNA respectively; similarly to the gel studies discussed previously in this chapter. Similar to the protection observed with AAPH and $Cu(OP)_2$, lanes 5-10 show that significant protection of the plasmid DNA from oxidative damage by Fenton reagent is also observed by condensing the plasmid with salmon protamine. At 0.5mM Fe(II), unpackaged DNA is sufficiently nicked to result in approximately 80% of the sample being in the open coiled state. Packaged DNA at the same iron concentration maintains ~80% in the supercoiled state. At 1mM Fe(II) unprotected DNA is primarily open coil with a small portion forming a

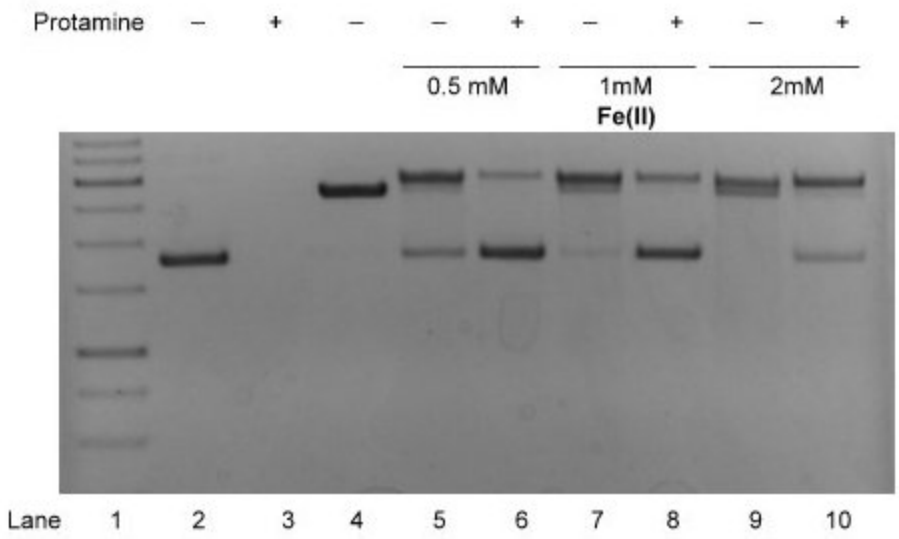

Figure 2.14 Packaged and unpackaged DNA's susceptibility to damage induced by fenton reactions. Lane 1 – 400ng of 1kb ladder; Lane 2 - 400ng of puc19 plasmid DNA; Lane 3 DNA condensed with protamine (N:P 2.0); Lane 4 - EcoR1 linearized DNA; Lane 5 - DNA treated with 0.5mM fenton reagent; Lane 6 – DNA packaged with protamine treated with 0.5mM fenton reagent; Lane 7 - DNA treated with 1.0mM fenton reagent; Lane 8 - DNA packaged with protamine treated with 1.0mM fenton reagent; Lane 9 – DNA treated with 2mM fenton reagent; Lane 10 – DNA packaged with protamine treated with 2mM fenton reagent.

linearized band. Protamine-DNA however shows no double strand breaks and still only a minor fraction nicked resulting in open coiled plasmid. Finally at 2mM Fe(II), unpackaged DNA appears to be linearized with a small amount remaining in the open coil band. Packaged DNA, in contrast, is primarily in the open coiled state with a small amount of supercoiled plasmid remaining. Similar to Cu(OP)2, some variation gel to gel for the exact amount of observed damage was seen with Fenton reagent. However,

undoubtedly packaged DNA offers more protection from oxidative damage than uncondensed DNA for all three free radical systems studied

Lastly, we examined Fenton reagents for K6, protamine, and R6 packaged DNA. These results are shown in figure 2.15. The degree of protection observed in figure 2.15 against 1 mM Fe(II) was less than in previous gels; which we attribute to the variation in free radical concentrations from gel to gel. In particular in this gel, the protection by protamine-DNA is less than observed in figure 2.14 above. However, when comparing protamine-DNA and R6-DNA to the more loosely packaged K6-DNA system, we again see improved protection arising from only a few angstroms of difference in the DNA-DNA spacings. Observing such differences in a low resolution method such as gel electrophoresis is still surprising and strongly suggests small changes in the packaging state may have dramatic effects on accrued mutagent damage in vivo in samples such as sperm chromatin. More experiments are needed to better resolve these sample to sample variations. In addition, we are exploring new means to better quantify ROS-like DNA damage then looking at supercoiled, open coiled and linear bands by gel electrophoresis.

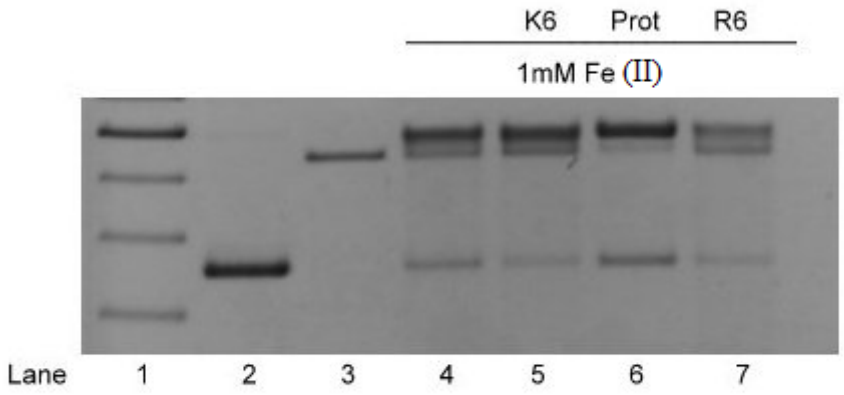

Figure 2.15 Various packaging states susceptibility to fenton reaction. Lane 1 – 400ng of 1kb Ladder; Lane 2 – 400ng Puc19 plasmid DNA; Lane 3 – EcoR1 linearized DNA; Lane 4 – DNA treated with 1.0mM fenton reagent; Lane 5 – DNA packaged with K6 (N:P 2.0) treated with 1.0mM fenton reagent Lane 6 – DNA packaged with protamine (N:P 2.0) treated with 1.0mM fenton reagent; Lane 7 – DNA packaged with R6 (N:P 2.0) treated with 1.0mM fenton reagent.

CHAPTER 3: EFFECTS OF UNDERPROTAMINATION ON DNA CONDENSATION AND DAMAGE

3.1 Introduction

As discussed in Chapter 1, to achieve the unique condensation state of sperm DNA must go through spermatogenesis; a dramatic cascade of events that include chromosome rearrangement through the replacement of histones with protamines [31]. In humans, sperm quality differs considerably between males as well as within a single ejaculate. Differences include not only sperm number, motility and morphology but also the manner in which chromatin is packaged [48]. We propose that one source of protamine dysfunction is the insufficient protamination in the sperm chromatin leading to defective sperm chromatin remodeling. Such mispackaging would then render the DNA more accessible to chemical agents that contribute significantly to DNA damage. Some experiments have established correlations between abnormal chromatin packaging and increased levels of DNA damage and higher percentage of underprotaminated sperm in some subjects Quantitative studies are hampered by the inherent difficulties of accurate protamine and DNA determinations in mammalian sperm cells. We propose that insufficient protamination in the sperm chromatin leads to defective sperm chromatin remodeling rendering the DNA more accessible to chemical agents that contribute significantly to DNA damage [49, 50]. To begin to test this hypothesis, this chapter will describe early experiments designed to examine DNA condensation by protamines at various nitrogen to phosphate (N:P) charge ratios. We show that even at low N:P ratios,

DNA can be at least partially condensed by protamine. Lastly, we show the effect of underprotamination on the protective capabilities of protamine to shield DNA from free radical damage. These experiments begin to provide insight into why protamine deficient nuclei are damaged.

3.1.1 N:P charge ratio

One of the key concepts for this Chapter is the nitrogen to phosphate (N:P) charge ratio. This concept is useful for concepts such as underprotamination and represents the balance of the negative charged phosphate residues of the DNA to the positively charged nitrogen resides on the various peptides used in this study. N:P ratios are also used in other fields, such as non-viral gene therapy, to describe the ratio of polycation to DNA phosphates in their gene vector formulations. N:P ratios below 1 indicate there is undercharging with more negative charged DNA residues than positively charged amino acids. N:P greater than 1 indicates an excess of positively charged amino acids in the mixing solution. This number is calculated by comparing the number of DNA base pairs (1 bp has two phosphates with an average bp molecular weight of ~ 660 g/mol) to the number of positively charged amino acids per sequence in solution. The number of positively charged amino acids was found by using a mass of 5125 g/mol for protamine chloride, with 21 positively charged residues

All cationic residues on salmon protamine used to neutralize DNA in protamine-DNA complexes are arginines. It has been previously shown by DeRouchey that arginine

peptides condense DNA to significantly higher packaging densities than comparably charged lysine peptides consist with the almost exclusive use of arginines in protamines [47]. In this Chapter, we will show gel retardation assays and UV/Vis results to examine DNA condensation at N:P ratios between 0 and 2. Early gel electrophoresis results on DNA damage as a function of N:P are also shown.

3.2 Methods and Materials

3.2.1 Materials

Ethidium bromide (EtBr) was purchased from Acros organics (Geel, Belgium). DNA puc19 plasmid was purchased from New England BioLabs (Ipswich, MA). 10X Phosphate buffer and Polyethlene Glycol 8K were purchased from Fisher Scientific. Protamine chloride from salmon (grade V histone free), Sodium azide (NaN_3), and Dextran Sulfate (DS) sodium salt, Calf Thymus were purchased from Sigma-Aldrich (St. Louis, MO). TAE buffer was purchased from Omega biotek (Norcross, GA). 3M sodium acetate was purchased from teknova (Hollister, CA). 1M tris buffer was purchased from cellgro (Tewksbury, MA).

3.2.2 Gel Preparation

Gels for the N:P retardation assay and DNA damage assessment were prepared in the same manner. Gels were cast in a 9 x 11 cm plastic plate with a ten lane comb. Each gel was made with 0.8% agarose solution, buffered with 1x TAE. Running Buffer solution was composed of 1X TAE solution. Current was applied to the gel with a FB300 power supply, purchased from Fischer Scientific. After electrophoresis, gel are stained in 2.5 μg/mL EtBr for 1 hour to allow visualization followed by a 30 min destain in 1x TAE. Gels were then imaged using a Fotodyne FOTO/Analyst Investigator/FX Workstation.

3.2.3 N:P gel retardation Assay

For the N:P gel retardation assay, agarose gels were prepared usually the following protocol. 400 nanograms of puc19 plasmid DNA was used per lane for all samples. Various amounts of protamine were added in order achieve the desired nitrogen to phosphate ratios. Buffer was added to maintain a total reaction volume of 10 μL per sample. Solutions were vortex to thoroughly mix and then spun down using a table-top centrifuge. Polycation-DNA mixtures were then incubated for 1 hour at room temperature to condense then samples. Following incubation, samples were centrifuged at 11000 x g for ten minutes. 1.5 μL of 6x loading buffer was then added to the resultant solution and

the solution was loaded onto a 0.8% agarose gel. Gel electrophoresis was conducted at 10 V/cm applied to the gel and run in 600mL of 1x TAE buffer. After 120 minutes, the gel was stained in 2.5 μg/mL ethidium bromide/1x TAE for one hour with shaking followed by a 30 min destain in 1x TAE before imaging.

3.2.4 N:P UV-Vis sample preparation

DNA concentration was checked by UV absorbance at 260 nm. It is known that for double stranded DNA, A260 = 1 corresponds to a DNA concentration 50 μg/L. We used grade V, histone free protamine chloride from salmon (Sigma Chemicals) and Type 1 calf-thymus DNA (Sigma Chemicals) was used for each UV absorbance experiment. The appropriate amount of protamine was added to DNA stock (850 mg/mL) to achieve the desired N:P ratio for 100μg and 75μg of DNA to a total volume of 250 μL and then incubated at room temperature for 1 hour. After incubation, samples were centrifuged at 11000 x g. 250 μL of the supernatant was then removed and placed in an Evolution UV-Visible Spectrometer from ThermoScientific to determine the A260 value from uncondensed DNA.

3.2.5 Sample Preparation for damage assays

To treat condensed sample with their respective damaging agent, the following steps were taken. Phosphate buffer, de-ionized water, protamine and puc19 plasmid DNA were mixed together. The amount of DNA was a constant 400 ng per sample, with varying levels of protamine added to achieve desired N:P ratio. The final concentration of phosphate buffer was 11.9mM, pH 7.4. Solutions were left to condense for a minimum of 15 minutes before being treated with their respective damaging agents (as outlined in 2.2.3 and 2.2.7).

Before loading, samples were mixed with 2 μL 6X loading buffer and 2 μL DS (15μg/μL). The 19 μL of solution were then loaded into the appropriate lanes on a 0.8% Agarose gel. Gel electrophoresis was conducted with 10 V/cm being applied to the gel. This was allowed to run in 600mL of 1x TAE buffer. After 120 minutes, gels were stained for one hour in 2.5 μg/mL ethidium bromide/1x TAE staining solution on a shaker. Gels were then destained in 1x TAE buffer for 30 minutes before imaging.

3.3 Results and Discussion

3.3.1 Resolution of agarose gels stained with ethidium bromide

We first wanted to establish the resolution of our ethidium bromide gel protocols. To do this, we electrophoresed various different amounts of puc19 plasmid DNA, stained

using our established protocol and imaged. The results are shown in Figure 3.1 with DNA concentrations ranging from 0 to 800 ng of plasmid DNA. The brightness of bands

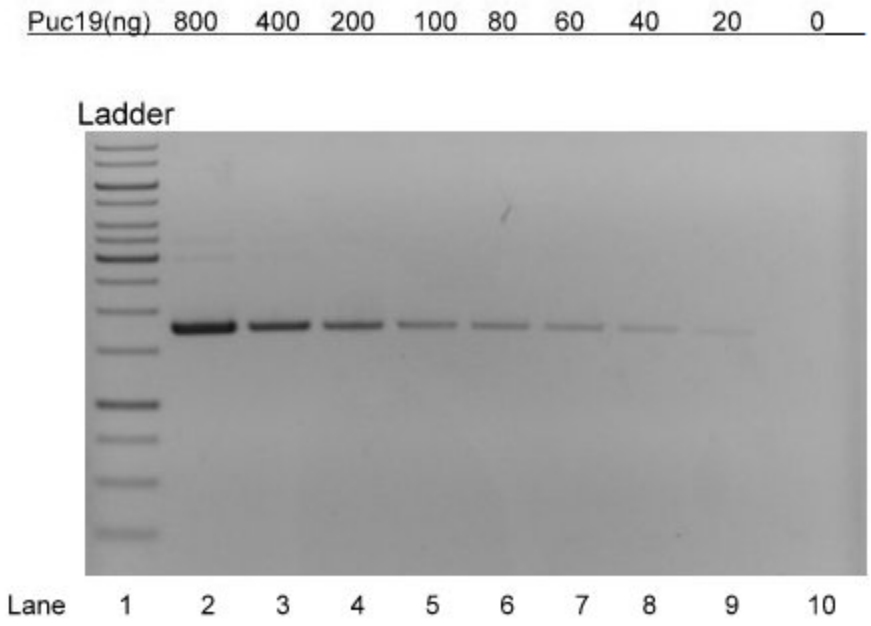

Figure 3.1 Depiction of DNA resolution detectable by UV light using Ethidium Bromide and Image Box to capture image. 400 ng of 1kb ladder loaded into gel lane one. Moving left to right puc19 plasmid was loaded in decreasing amounts; lane 2 – 800 ng of DNA, lane 3 – 400 ng of DNA, lane 4 – 200 ng of DNA, lane 5 – 100 ng of DNA, lane 6 – 80 ng of DNA, lane 7 – 60 ng of DNA, lane 8 – 40 ng of DNA, lane 9 – 20 ng of DNA, lane 10 – 0 ng of DNA.

directly correlates to the amount of DNA within the band. All DNA concentrations tested gave rise to at least one band corresponding to the supercoiled plasmid state. A very faint band is detected at the lowest DNA concentration (20 ng) roughly establishing the resolving power of our gel protocol. For the following experiments, a constant amount of

400 ng of DNA was used per well. Figure 3.1 suggests that we can resolve approximately 5% changes in the total DNA concentration. Lane 10 had no DNA loaded and no bands are observed. This is shown to establish that no contamination was present.

3.3.2 Gel retardation assay of protamine-DNA at varying N:P charge ratios

Next we wanted to examine the DNA condensation at various N:P charge ratios using a gel retardation assay. Such assays are commonly used for polycation-DNA, or polyplex, formulations used in non-viral gene therapy to establish full condensation of the plasmid DNA of interest. Results for salmon protamine-DNA are shown in Figure 3.2 as a function of increasing N:P charge ratio. Here protamine-DNA was mixed at the desired N:P charge ratio, incubated for 1 hour, then loaded onto the gel. Complexed DNA is both charge neutralized and thought to form nanoparticles too large to penetrate into the gel resulting in a decrease of DNA observed as a function of the degree of condensation. Figure 3.2 shows clear evidence of the disappearance of the supercoiled DNA band with increasing protamine concentration. Some smearing is observed presumably arising due to weak interactions between the protamine and DNA in

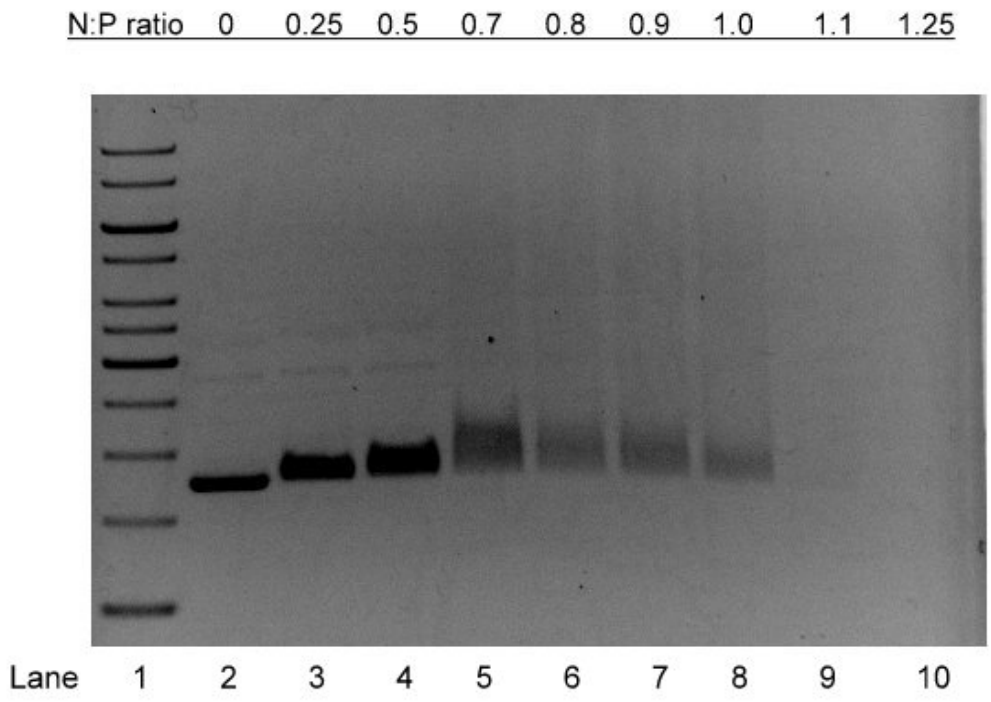

Figure 3.2 N:P gel Assay. The amount of protamine is increased from left to right across the gel while DNA amount remains the same; lane 1 – Ladder, lane 2 – 400ng of puc19 plasmid, lane 3 – N:P 0.25, lane 4 – N:P 0.5, lane 5 – N:P 0.7, lane 6 – N:P 0.8, lane 7 – N:P 0.9, lane 8 – N:P 1.0, lane 9 – N:P 1.1, lane 10 – N:P 1.2

undercharged systems. A faint band is observed at N:P 1.0 but by N:P 1.1 all DNA is observed to be fully condensed (or at least less than 20 ng of DNA is unbound). This is consistent with the arginines of protamine being fully charged at neutral pH and the strong interactions of the peptide with DNA.

3.3.3 UV-Vis experiments of DNA condensation by salmon protamine

We also examined DNA condensation by salmon protamine using UV-Vis experiments. Figure 3.3 shows the normalized A260 plotted as a function of increasing N:P ratio. Even at very high degrees of underprotamination (e.g. N:P 0.25), we see a significant decrease in the A260 corresponding to some fraction of the DNA being condensed. With increasing N:P ratio, the A260 continues to decrease reaching ~ 0 at N:P

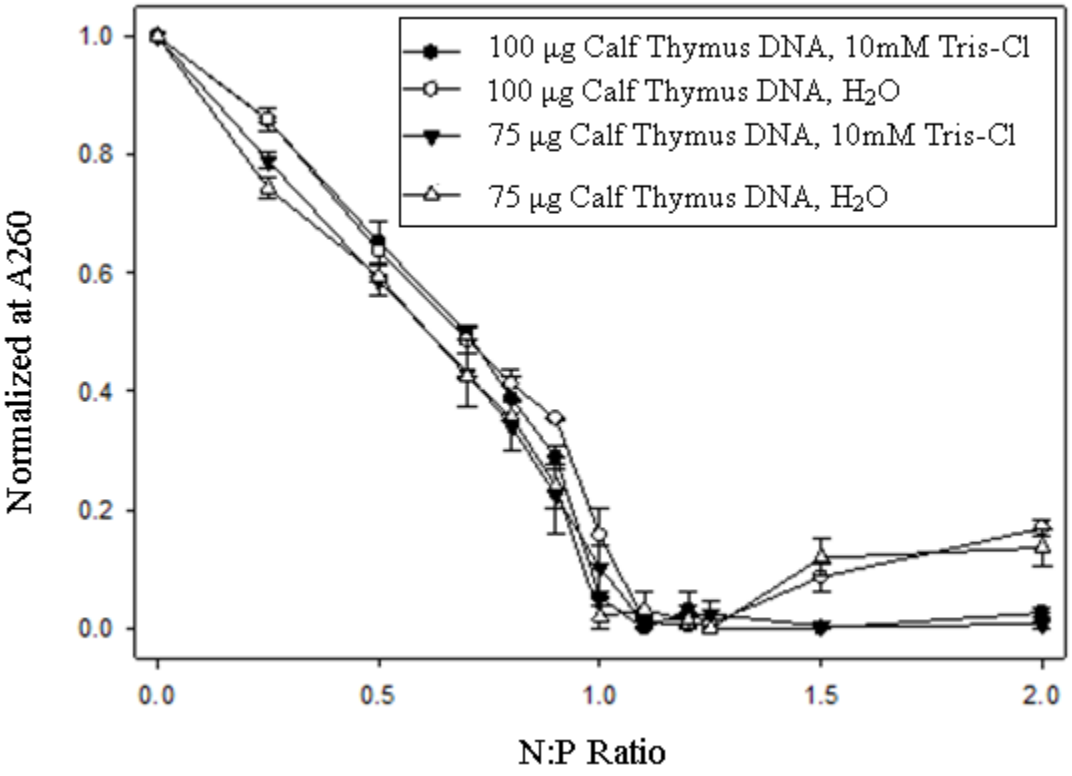

Figure 3.3 UV-Vis Studies of DNA condensation at Multiple N:P ratios

*The work contained in this chapter is being prepared for publication as:

Characterization of Protamine-DNA packaging, influence of N:P ratio

Daniel Kirchhoff, Cody Gay, Ehigbai Oikeh and Dr. Jason DeRouchey

Department of Chemistry, University of Kentucky, Lexington, KY, 40506-0055

1.0 for both DNA in distilled water as well as 10 mM TrisCl (pH 7.5) buffer. These results are in agreement with our gel retardation assays in Figure 3.2 showing a 1:1 charge ratio is sufficient to fully condense the DNA. Interestingly, a small fraction of DNA appears to be free at higher N:P ratios in pure water. It is not clear why this would happen and this is not observed in the presence of Tris buffer.

3.3.4 DNA Damage assays for underprotaminated DNA

In this section, we have utilized the DNA damage gel assays discussed in Chapter 2 to investigate DNA damage as a function of N:P charge ratios using both AAPH and Fenton reagent as our free radical damaging source. Figures 3.4 & 3.5 show initial damage gel results at 200μM and 1 mM AAPH, respectively, as a function of increasing protamine concentration. These concentrations represent a "low" and "high" degree of damage to unpackaged DNA as observed in Chapter 2. 400 ng per well was maintained for all samples. After condensation, all samples were exposed to AAPH for 1 hour. Then a decondensing agent (dextran sulfate) was added and the samples immediately loaded onto the gels for analysis. Both gels show increased protection afforded by the presence of higher amounts of protamine. Unpackaged DNA is seen to be almost entirely nicked at 200μM AAPH with only the open coiled DNA band observed in Figure 3.4. By 1.0 mM AAPH, unpackaged DNA is approximately 50% open coil and 50% linearized as seen in lane 4 of Figure 3.5. Once above N:P 1.0, the protection appears to be maximized and is similar to the protection observed at N:P 2.0 observed in previous gels discussed in

Chapter 2. This increased protection is most evident at N:P 1.1 where significant amounts of supercoiled DNA is regained in Figure 3.4 and open coiled DNA in Figure 3.5. The conversion from a more damaged band to a less damaged band indicates that the more packaged the DNA the more protected the DNA is from oxidative damage. This packaging protection is maximized at N:P 1.0. More gel work needs to be done to establish the reproducibility of these results. In addition, currently SAXS experiments are underway to examine the DNA-DNA interaxial spacings as a function of increasing salmon protamine concentration. We hypothesize that DNA-DNA spacings are minimal at N:P 1.0 and no further packaging will commence with the addition of excess protamine.

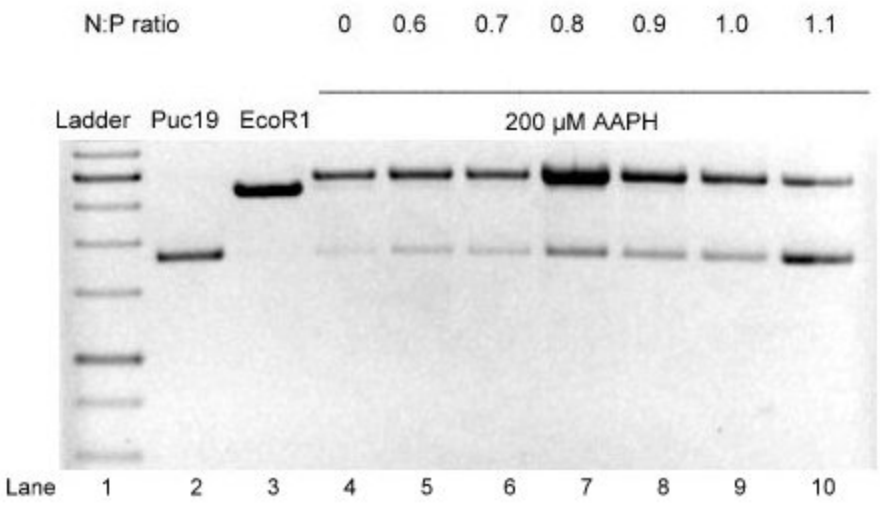

Figure 3.4 Various N:P ratios susceptibility to lower concentrations of AAPH. Lane 1 – 1kb Ladder, Lane 2 – 400ng puc19 plasmid DNA; Lane 3 – EcoR1 linearized DNA, Lane 4 DNA treated with 200µM AAPH; Lane 5 – DNA packaged with protamine, N:P 0.6, treated with 200µM AAPH; Lane 6 - DNA packaged with protamine, N:P 0.7, treated with 200µM AAPH; Lane 7 - DNA packaged with protamine, N:P 0.8, treated with 200µM AAPH; Lane 8 - DNA packaged with protamine, N:P 0.9 treated with 200µM AAPH; Lane 9 - DNA packaged with protamine, N:P 1.0 treated with 200µM AAPH; Lane 10 - DNA packaged with protamine, N:P 1.1 treated with 200µM AAPH.

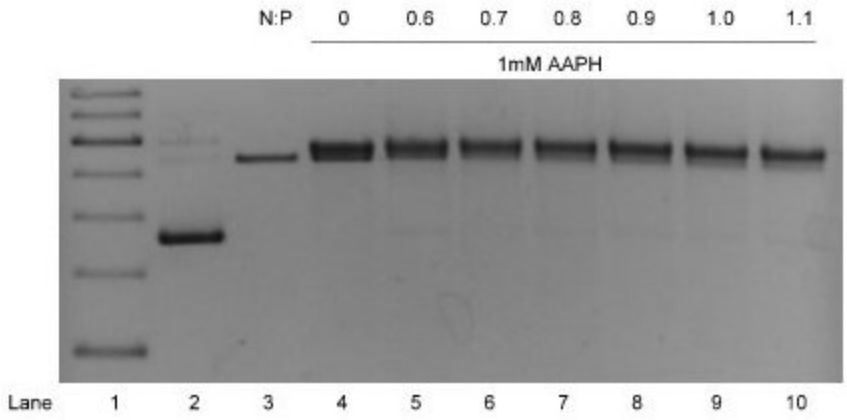

Figure 3.5 Various N:P ratios susceptibility to higher levels of AAPH. Lane 1 – 1kb Ladder; Lane 2 – 400ng puc19 plasmid DNA; Lane 3 – EcoR1 linearized DNA; Lane 4 DNA treated with 1mM AAPH; Lane 5 – DNA packaged with protamine, N:P 0.6 treated with 1mM AAPH; Lane 6 - DNA packaged with protamine, N:P 0.7 treated with 1mM AAPH; Lane 7 - DNA packaged with protamine, N:P 0.8 treated with 1mM AAPH; Lane 8 - DNA packaged with protamine, N:P 0.9 treated with 1mM AAPH; Lane 9 - DNA packaged with protamine, N:P 1.0 treated with 1mM AAPH; Lane 10 - DNA packaged with protamine, N:P 1.1 treated with 1mM AAPH.

Lastly, we examined the susceptibility of DNA to be damaged as a function of the N:P charge ratio using Fenton reagent. Shown in Figure 3.6 is gel electrophoresis results of puc19 plasmid with increasing salmon protamine chloride concentration exposed to 1 mM Fe(II) concentration. Lanes 1, 2, and 3 are included as control lanes including a 1kbp ladder, unmodified puc19 plasmid and EcoRI linearized puc19 respectively. Lane 4 shows that unpackaged DNA exposed to 1mM Fenton shows considerable damage with nearly all the sample being in the open coiled state and small amounts of linearized DNA also observed. Clearly the Fenton reagent at this concentration is efficient in generating single strand nicks and even double strand breaks. Salmon protamine was added to

generate protamine-DNA samples with N:P between 0.6 and 1.1. Only mild protection, at best, is observed in this experiment with increasing protamine concentration. From lane 5 to lane 10, there is a small increase in the fraction of supercoiled DNA observed at the bottom of the gel. We note that the protection observed at N:P 1.1 is not as great to that observed at N:P 2 shown in figures 2.7, 2.8, 2.13, and 2.14 in Chapter 2. More work needs to be done to better establish the protective capacity of salmon protamine to Fenton reagent as a function of increasing N:P ratio. In particular if this protection varies between AAPH and Fenton chemistries.

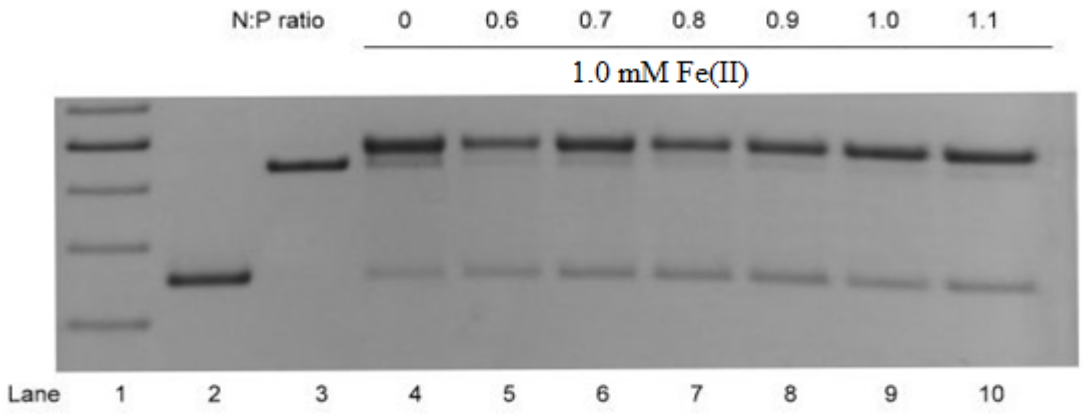

Figure 3.6 Various N:P ratios susceptibility to damage induced by fenton reaction. Lane 1 – 1kb Ladder; Lane 2 – 400ng puc19 plasmid DNA; Lane 3 – EcoR1 linearized DNA; Lane 4 DNA treated with 1mM fenton reagent; Lane 5 – DNA packaged with protamine, N:P 0.6 treated with 1mM fenton reagent; Lane 6 - DNA packaged with protamine, N:P 0.7 treated with 1mM fenton reagent; Lane 7 - DNA packaged with protamine, N:P 0.8 treated with 1mM fenton reagent; Lane 8 - DNA packaged with protamine, N:P 0.9 treated with 1mM fenton reagent; Lane 9 - DNA packaged with protamine, N:P 1.0 treated with 1mM fenton reagent; Lane 10 - DNA packaged with protamine, N:P 1.1 treated with 1mM fenton reagent.

CHAPTER FOUR: CONCLUSIONS AND FUTURE DIRECTIONS

4.1 Conclusion

The search for infertility causes and treatments is still lacking in answers. While the majority of infertility caused by males can be traced back to low sperm count or motility issues; it is known that a significant fraction is associated with abnormal sperm chromatin packaging. Routine clinical examinations do not identify subtle defects in sperm chromatin architecture. Better understanding of effective sperm chromatin remodeling is especially important with the vast increases of assisted reproductive techniques (ART) in recent years where the quality of the selected sperm is of utmost importance. ART in the US has more doubled over the last ten years. While assays such as COMET and TUNEL have been developed to qualitatively assess DNA fragmentation within sperm cells; there is still a need for a more quantitative understanding of the link between DNA packaging and DNA damage. In this thesis, we have used biophysical and biochemical methods to better understand the link between cation packaging of DNA and the protective capabilities of packaging from oxidative damage.

4.1.1 DNA Damage in packaged and unpackaged DNA

In Chapter 2, we focused on three main questions: (1) Does condensed DNA protect DNA from oxidative damage from free radicals (2) Can we quantify this

protection? and (3) do small changes in the packaging density affect the capacity to protect nucleic acids in condensates? In answering these questions, we primarily used gel electrophoresis to visualize differences in the supercoiled, open coiled and linear bands observed when running puc19 plasmid DNA. DNA was damaged using one of three possible free radical sources; AAPH, Copper phenanthroline (Cu(OP)2) or Fenton reagent.

Figures 2.6, 2.10, and 2.13 show the concentration dependence of damaged to unpackaged DNA using AAPH, Cu(OP)2 or Fenton reagent, respectively. All three free radical systems show a systematic increase in the amount of damage as a function of increasing free radical concentration. This increased damage was assessed by increasing amounts of nicked, linearized, or degraded DNA, as a function observed in the gel. Once we had established the free radical concentration range of interest to achieve low to high amounts of damage to naked DNA, we then examined if condensed DNA did enable protection of the nucleic acid bases from oxidative damage. Figure 2.7, 2.11, and 2.14 show side-by-side comparisons of naked DNA and DNA fully condensed by salmon protamine exposed to various concentrations of AAPH, Cu(OP)2 or Fenton reagent, respectively. For all three systems, significant differences were observed between the free and packaged state at all free radical concentrations examined. As expected, protamine condensed DNA shows significant improved stability when compared to unpackaged DNA. We attribute this improved stability to the reduced accessibility of the bases to the free radical species in the condensed state. Lastly, we investigated how different condensed states affect the ability of free radicals to damage DNA. Building on prior

knowledge from the DeRouchey lab, we used hexalysine and hexaarginine peptides to compare to protamine DNA. R6-DNA and salmon protamine-DNA result in similar packaging with an interaxial DNA-DNA spacing of 28.6 Å and 29.3 Å, respectively. K6-DNA is known to have a significantly reduced packaging density with an equilibrium DNA-DNA spacing of 32.3 Å. Figure 2.9, 2.12, and 2.15 show a side by side comparison of these packaged states exposed to a constant concentration of AAPH, Cu(OP)2 or Fenton reagent. In all three damaging systems, the K6-DNA is observed to have significantly less protective capacity when compared to R6 and protamine condensed DNA. Interestingly, although the R6-DNA is known to condense to slightly smaller DNA-DNA spacings, the protamine-DNA system seems to consistently show better DNA stability. This may be due to kinetic issues arising from the higher charge, and greater length, of the protamine and thus higher affinity for DNA.

4.1.2 Characterization of Underprotamination on condensation and damage of DNA

It is known that in some humans, higher abnormal chromatin packaging is associated with observed higher rates of DNA damage and higher percentages of underprotamination. We propose, therefore, that insufficient protamination in the sperm chromatin leads to defective sperm chromatin remodeling rendering the DNA more accessible to chemical agents that contribute significantly to DNA damage. Chapter 3 describes early experiments to better elucidate the role of underprotamination on both the ability of DNA to condense and package DNA as well as protect it from free radical

attack. Chapter 3 shows DNA condensation by gel retardation assays and UV-Vis absorption experiments as a function of increasing protamine concentration. The ratio of DNA to protamine is given as a nitrogen to phosphate (N:P) charge ratio of the number of positively charged amino groups from the arginines of salmon protamine to the number of negatively charged phosphate groups on the DNA. Both gel retardation and UV-Vis clearly shows that protamine is capable of condensing DNA even at low N:P ratios. This condensation continues to proceed to a greater extent with the addition of more protamine reaching full condensation at charge ratios of 1. As expected, at N:P > 1, all the DNA is fully condensed due to a complete charge compensation between the protamine and DNA polymers. DNA damage gel assays were also performed to examine the extent of damage as a function of the N:P ratio. AAPH and Fenton reagent were both examined as the free radical source. Our early results show increased protection in both systems as the N:P ratio reaches 1. The observed protection is much higher in the AAPH system as compared to the Fenton reagent but more work needs to be done to assess the reproducibility of these gels. From previous work, we anticipate that the DNA-DNA spacings will change greatly for underprotaminated samples but then reach a minimum at N:P 1.0. Currently small-angle x-ray (SAXS) experiments are being performed in the DeRouchey lab to examine this hypothesis and quantify the effects of underprotamination on the DNA-DNA spacings in the condensates. We believe these experiments may begin to provide direct insight into why protamine deficient nuclei are damaged.

4.2 Future Directions

The gel methods used in our study are relatively simplistic methods. We quantify DNA damage by comparing how much plasmid is left in the supercoiled state compared to DNA with single strand breaks, double strand breaks, and fragmented DNA. The free radical concentrations required to induce double strand breaks are very high and well above expected ROS levels in vivo. Images produced by gel electrophoresis cannot provide information about oxidized sample. For example, the amount of oxidized bases, or abasic sites is not known. It is known in vivo that damage to DNA in this way can lead to mispairing, deletions, and genetic mutations. Long-term, we would like to find means to examine ROS damage and quantify the amount of oxidized bases for DNA in various packaged states.

One possible approach to investigate this problem would be selecting a damage biomarker and the rates of its appearance after damaging. 8-hydroxy-2' -deoxyguanosine (8-OHdG) is one of the more predominant biomarkers that arise from oxidative damage with free radicals. The base 8-OHdG is derived from, Guanine, is very susceptible to oxidative damage because of its relatively high oxidation potential [51]. For this reason, 8-OHdG is known to be an important marker for analyzing quantitatively the amount of damage to ROS exposed DNA. Testing the amount of 8-OHdG present in a sample on a mass spectrometer (MS) would be an excellent way to determine the amount of protection offered in a DNA sample. Work on this approach has been started by our lab in the past. Trouble arose with the timing of the sample damage to when samples could

be processed by the MS facility as well as with the sample optimization for MS studies. Future studies will have to develop a protocol to systematically quench a sample in a way that doesn't interfere with the operations of a MS. Future work will also have to develop a protocol to remove metals from the damaging process before the samples are tested.

REFERENCES

1. Wyrobek, A., et al., *Physical characteristics of mouse sperm nuclei.* Biophysical journal, 1976. **16**(7): p. 811.
2. Ward, W.S. and D. Coffey, *DNA packaging and organization in mammalian spermatozoa: comparison with somatic cells.* Biology of reproduction, 1991. **44**(4): p. 569-574.
3. Miller, D., *Confrontation, Consolidation, and Recognition: The Oocyte's Perspective on the Incoming Sperm.* Cold Spring Harbor Perspectives in Medicine, 2015. **5**(8).
4. McGhee, J. and G. Felsenfeld, *Nucleosome structure.* Annual review of biochemistry, 1980. **49**(1): p. 1115-1156.
5. Ward, W.S., *Function of sperm chromatin structural elements in fertilization and development.* Molecular human reproduction, 2010. **16**(1): p. 30-36.
6. Johnson, G.D., et al., *The sperm nucleus: chromatin, RNA, and the nuclear matrix.* Reproduction, 2011. **141**(1): p. 21-36.
7. Daly, M.M., A.E. Mirsky, and H. Ris, *THE AMINO ACID COMPOSITION AND SOME PROPERTIES OF HISTONES.* The Journal of General Physiology, 1951. **34**(4): p. 439-450.
8. Balhorn, R., *The protamine family of sperm nuclear proteins.* Genome Biology, 2007. **8**(9): p. 227-227.
9. Bloomfield, V.A., *DNA condensation by multivalent cations.* Biopolymers, 1997. **44**(3): p. 269-282.
10. Bloomfield, V.A., *DNA condensation.* Current opinion in structural biology, 1996. **6**(3): p. 334-341.
11. Hud, N.V., F.P. Milanovich, and R. Balhorn, *Evidence of novel secondary structure in DNA-bound protamine is revealed by Raman spectroscopy.* Biochemistry, 1994. **33**(24): p. 7528-7535.
12. DeRouchey, J.E. and D.C. Rau, *Role of Amino Acid Insertions on Intermolecular Forces between Arginine Peptide Condensed DNA Helices IMPLICATIONS FOR PROTAMINE-DNA PACKAGING IN SPERM.* Journal of Biological Chemistry, 2011. **286**(49): p. 41985-41992.
13. Green, G., et al., *Synthesis and processing of mammalian protamines and transition proteins.* Molecular reproduction and development, 1994. **37**(3): p. 255-263.
14. Amann, R.P., *The cycle of the seminiferous epithelium in humans: a need to revisit?* Journal of andrology, 2008. **29**(5): p. 469-487.
15. Forster, P., et al., *Elevated germline mutation rate in teenage fathers.* Proceedings of the Royal Society of London B: Biological Sciences, 2015. **282**(1803): p. 20142898.
16. Allahbadia, G.N. and R.B. Das, *The art and science of assisted reproductive techniques*. 2004: CRC Press.
17. *Anatomy and Physiology of the Male Reproductive System*. [cited 2016; Available from: https://legacy.cnx.org/content/m46400/1.3/?legacy=true.

18. Staff, M.C. *Male infertility*. 2015 6-3-2016]; Available from: http://www.mayoclinic.org/diseases-conditions/male-infertility/basics/definition/con-20033113.
19. Hammadeh, M., et al., *Protamine contents and P1/P2 ratio in human spermatozoa from smokers and non-smokers.* Human Reproduction, 2010. **25**(11): p. 2708-2720.
20. Venkatesh, S., et al., *Clinical significance of sperm DNA damage threshold value in the assessment of male infertility.* Reproductive Sciences, 2011. **18**(10): p. 1005-1013.
21. Wright, C., S. Milne, and H. Leeson, *Sperm DNA damage caused by oxidative stress: modifiable clinical, lifestyle and nutritional factors in male infertility.* Reproductive biomedicine online, 2014. **28**(6): p. 684-703.
22. Lewis, S.E., *The place of sperm DNA fragmentation testing in current day fertility management.* Middle East Fertility Society Journal, 2013. **18**(2): p. 78-82.
23. Kumar, K., et al., *Predictive value of DNA integrity analysis in idiopathic recurrent pregnancy loss following spontaneous conception.* Journal of assisted reproduction and genetics, 2012. **29**(9): p. 861-867.
24. Cocuzza, M., et al., *Clinical relevance of oxidative stress and sperm chromatin damage in male infertility: an evidence based analysis.* International braz j urol, 2007. **33**: p. 603-621.
25. Valko, M., et al., *Free radicals and antioxidants in normal physiological functions and human disease.* The international journal of biochemistry & cell biology, 2007. **39**(1): p. 44-84.
26. Alvarez, J.G., et al., *Spontaneous lipid peroxidation and production of hydrogen peroxide and superoxide in human spermatozoa. Superoxide dismutase as major enzyme protectant against oxygen toxicity.* J androl, 1987. **8**(5): p. 338-48.
27. De Lamirande, E., P. Leclerc, and C. Gagnon, *Capacitation as a regulatory event that primes spermatozoa for the acrosome reaction and fertilization.* Molecular Human Reproduction, 1997. **3**(3): p. 175-194.
28. Oehninger, S., et al., *Effects of hydrogen peroxide on human spermatozoa.* Journal of assisted reproduction and genetics, 1995. **12**(1): p. 41-47.
29. Conrad, M., et al., *The nuclear form of phospholipid hydroperoxide glutathione peroxidase is a protein thiol peroxidase contributing to sperm chromatin stability.* Molecular and cellular biology, 2005. **25**(17): p. 7637-7644.
30. Aitken, R. and G. De Iuliis, *On the possible origins of DNA damage in human spermatozoa.* Molecular human reproduction, 2010. **16**(1): p. 3-13.
31. Leduc, F., G.B. Nkoma, and G. Boissonneault, *Spermiogenesis and DNA repair: a possible etiology of human infertility and genetic disorders.* Systems biology in reproductive medicine, 2008. **54**(1): p. 3-10.
32. González-Marín, C., J. Gosálvez, and R. Roy, *Types, causes, detection and repair of DNA fragmentation in animal and human sperm cells.* International journal of molecular sciences, 2012. **13**(11): p. 14026-14052.
33. Werber, J., et al., *Analysis of 2, 2'-azobis (2-amidinopropane) dihydrochloride degradation and hydrolysis in aqueous solutions.* Journal of pharmaceutical sciences, 2011. **100**(8): p. 3307-3315.

34. Purcell, M., *Obtaining thylakoids from photosynthetic organisms; plant fractions obtained from the process; pure thylakoids; and methods of use of thylakoids as ros scavengers, photo-protectors, biosensors, biofilters and bioreactors*. 2003, Google Patents.
35. Betigeri, S., A. Thakur, and K. Raghavan, *Use of 2, 2'-azobis (2-amidinopropane) dihydrochloride as a reagent tool for evaluation of oxidative stability of drugs.* Pharmaceutical research, 2005. **22**(2): p. 310-317.
36. Shao, J., N.E. Geacintov, and V. Shafirovich, *Oxidative Modification of Guanine Bases Initiated by Oxyl Radicals Derived from Photolysis of Azo Compounds.* The Journal of Physical Chemistry B, 2010. **114**(19): p. 6685-6692.
37. Bales, B.C., et al., *Mechanistic studies on DNA damage by minor groove binding copper–phenanthroline conjugates.* Nucleic acids research, 2005. **33**(16): p. 5371-5379.
38. Dai, Z. and C. Wu, *How Does DNA Complex with Polyethylenimine with Different Chain Lengths and Topologies in Their Aqueous Solution Mixtures?* Macromolecules, 2012. **45**(10): p. 4346-4353.
39. Lee, P.Y., et al., *Agarose Gel Electrophoresis for the Separation of DNA Fragments.* J Vis Exp, 2012(62).
40. FH, K., *Overview of agarose gel properties. Electrophoresis of large DNA molecules: theory and applications.* 1991.
41. EJ, D., *IDT tutorial: gel electrophoresis*. 2010.
42. Meyers, J.A., et al., *Simple agarose gel electrophoretic method for the identification and characterization of plasmid deoxyribonucleic acid.* Journal of bacteriology., 1976. **127**(3): p. 1529-1537.
43. Vinograd, J., et al., *The twisted circular form of polyoma viral DNA.* Proceedings of the National Academy of Sciences, 1965. **53**(5): p. 1104-1111.
44. Patterton, H.-G. and C. von Holt, *Negative Supercoiling and Nucleosome Cores: I. The Effect of Negative Supercoiling on the Efficiency of Nucleosome Core Formation in Vitro.* Journal of molecular biology, 1993. **229**(3): p. 623-636.
45. Calladine, C.R. and H. Drew, *Understanding DNA: the molecule and how it works*. 1997: Academic press.
46. Champoux, J.J., *DNA topoisomerases: structure, function, and mechanism.* Annual review of biochemistry, 2001. **70**(1): p. 369-413.
47. DeRouchey, J., B. Hoover, and D.C. Rau, *A Comparison of DNA Compaction by Arginine and Lysine Peptides: A Physical Basis for Arginine Rich Protamines.* Biochemistry, 2013. **52**(17): p. 3000-3009.
48. Manicardi, G.C., et al., *DNA strand breaks in ejaculated human spermatozoa: comparison of susceptibility to the nick translation and terminal transferase assays.* The Histochemical Journal, 1998. **30**(1): p. 33-39.
49. Bianchi, P., et al., *Effect of deoxyribonucleic acid protamination on fluorochrome staining and in situ nick-translation of murine and human mature spermatozoa.* Biology of Reproduction, 1993. **49**(5): p. 1083-1088.
50. Esterhuizen, A., et al., *Chromatin packaging as an indicator of human sperm dysfunction.* Journal of assisted reproduction and genetics, 2000. **17**(9): p. 508-514.

51. Neeley, W.L. and J.M. Essigmann, *Mechanisms of formation, genotoxicity, and mutation of guanine oxidation products.* Chemical research in toxicology, 2006. **19**(4): p. 491-505.

Cody Gay

EDUCATION

Bachelor of Science in Chemistry, University of the Cumberlands, Williamsburg, KY, 2009-2013

PUBLICATIONS

Characterization of Protamine-DNA packaging, influence of N:P ratio
Daniel Kirchhoff, Cody Gay, Ehigbai Oikeh and Dr. Jason DeRouchey
Department of Chemistry, University of Kentucky, Lexington, KY, 40506-0055
Preparing for publication.

Polycation mediated protection of DNA from indirect DNA damage by free radicals
Cody Gay, Daniel Kirchhoff, Ehigbai Oikeh and Dr. Jason DeRouchey
Department of Chemistry, University of Kentucky, Lexington, KY, 40506-0055
Preparing for publication.

PROFESSIONAL POSITIONS

Research Assistant at the University of Kentucky, Department of Chemistry, Lexington KY, 2014-2016

Teaching Assistant at the University of Kentucky, Department of Chemistry, Lexington KY, 2014-2016